



Norwegian University of
Science and Technology

Air return in brook intake shafts.

Stefan Perzyna

Master of Science in Civil and Environmental Engineering

Submission date: July 2017

Supervisor: Leif Lia, IBM

Norwegian University of Science and Technology
Department of Civil and Environmental Engineering

Preface

This thesis was prepared as a part of Master of Science Program in Hydraulic Engineering held at the Water and Environment Institute at Norwegian University of Science and Technology in Trondheim. The primary goal of the project was to investigate the effects of air accumulation in tunnel systems, particularly the phenomenon of air movement in inclined conduits. We hope that the results of this project may contribute to the improvement of a design guidance for brook intakes with regard to air blowouts prevention.

A laboratory experiment was carried out in the Hydraulic Laboratory of the Trondheim Norwegian University of Science and Technology.

I would like to thank my tutors, prof. Leif Lia and Morten Skoglund for their wise council and valuable suggestions. I am grateful to the staff members of the Hydraulic Laboratory for their great support with the building of the model and many practical pieces of advice. Finally, I would like to thank my parents for their support throughout my studies.

Stefan Perzyna

Trondheim, Norway

July 2017

Summary

In Norwegian practice, it is common to construct additional intakes (brook intakes) to collect the water from smaller streams and transport the water to the reservoir to increase the production of a hydropower plant. Undesired air entrainment can lead to head loss, supersaturation in downstream water or harmful blowouts in these intakes. Therefore, it is essential to try to understand the air transport phenomena in inclined conduits in order to provide guidance in brook intakes design and operation that would prevent hazardous blowouts from these intakes.

Experimental studies were conducted in order to understand the phenomenon of air movement and air accumulation in the inclined conduits that can lead to blowouts in brook intakes. A physical model was built in the laboratory for this purpose. The model included a circular shaft with diameter 210 mm connected to a horseshoe shaped tunnel with dimensions 400 mm x 400 mm. Tests were performed for three model configurations with the 45⁰, 60⁰ and 90⁰ inclined shafts.

Detailed investigations of the flow patterns in the shaft and flow conditions in the tunnel were performed. It was concluded that a prerequisite for a blowout to occur is a change of flow regime and formation of air pockets in the intake shaft. This happens for conditions at which air can accumulate in the tunnel. Results of experiments allowed for determination of threshold velocities for the continuous air return and for the beginning of air accumulation in the tunnel. A threshold velocity for the continuous air return is considered a limiting velocity for an occurrence of hazardous blowouts.

Table of contents

Preface.....	i
Summary	iii
Table of contents	iv
Figure list.....	v
Table list.....	vi
Symbols.....	vii
Terminology.....	viii
1 Introduction.....	1
1.1 Problem statement and methodological approach.....	2
1.2 Structure of the Master thesis	2
2 Theoretical background and literature overview.....	3
2.1 Two-phase flow	3
2.2 Air and water flow in downward-sloping pipes	5
2.3 Literature review.....	9
3 Laboratory experiment.....	19
3.1 Dimensional analysis.....	19
3.2 Model scaling issues.....	20
3.3 Design of the model.....	20
3.4 Testing facility and instrumentation description	22
3.5 Experiment procedure.....	26
4 Test results and observations.....	28
4.1 Flow patterns observed in the shaft	28
4.2 Frequency of air return	32
4.3 Observations in the tunnel	35
4.4 Determining dimensionless velocities	37
4.5 Comparison of Flow numbers for different model setup	42
4.6 Scaling of results	44
4.7 Comparison with prototypes.....	45
4.8 Test method review	46
5 Conclusions	48
5.1 Final conclusions	48
5.2 Recommendation for further research	49
6 Bibliography.....	51
Appendix A- Example of observations for 45 ⁰ shaft	53
Appendix B- Additional model pictures	55
Appendix C- Model design sketches.....	57
Appendix D- Air discharge curve	59
Appendix E- Master Thesis contract.....	60

Figure list

Figure 1-Outblow at Holmaliåna brook intake (Bekkeinntakskomiteen, 1986).....	1
Figure 2-Flow regimes occurring in horizontal pipes, (Weisman, 1983), (Palsson, n.d.)	4
Figure 3 Flow regimes occurring in the vertical pipes (Weisman, 1983).....	4
Figure 4 Air entrainment in Brook intake shaft (Berg, 1986).....	5
Figure 5 Forces acting on air bubble (Falvey, 1980)	6
Figure 6 Return Flow (Berg, 1986).....	8
Figure 7 Air pocket (Berg, 1986).....	8
Figure 8- Air transport in closed conduit (Falvey, 1980).....	11
Figure 9 Critical flow numbers depending on pipe slope (Pothof, 2011)	12
Figure 10 Air movement in downward-sloping pipes (Pozos, et al., 2010).....	13
Figure 11 -Threshold velocity for continuous return of air (Berg, 1986)	14
Figure 12-Results from a research with direct connection of shaft to the tunnel (Dahl & Guttormsen, 1986).....	15
Figure 13 Experiment setup by Berg (Berg, 1986)	16
Figure 14-Experiment setup by Gjerde (Utvik Gjerde, 2009)	16
Figure 15- Brook intake model with the 60 ⁰ shaft.....	22
Figure 16-Water tank, view from above.	23
Figure 17- Outflow regulation with a butterfly valve	23
Figure 18- Model setup for 45, 60, 90 degrees.	24
Figure 19- Water provision to the model	25
Figure 20 Air flow meter.....	25
Figure 21-Type 3 flow regime, 45 ⁰ minimum air, 30l/s.....	30
Figure 22-Type 4 regime, 45 ⁰ , 1.3% air, 30l/s, bubble is closing.....	30
Figure 23-Type 4 regime, 45 ⁰ , minimum air, 40l/s.....	30
Figure 24-Type 5 regime, 45 ⁰ ,1.3% air, 40l/s	30
Figure 25 Pocket propagation in vertical shaft (Flow pattern 7).....	32
Figure 26-Air return frequency in 45 ⁰ shaft.....	33
Figure 27-Air return frequency in 60 ⁰ shaft.....	34
Figure 28-Air return frequency in 90 ⁰ shaft.....	34
Figure 29-Standing pocket in the tunnel	36
Figure 30-Standing pocket expanding to the shaft.....	36
Figure 31- Air accumulation in tunnel with 60 ⁰ shaft.....	36
Figure 32- Air accumulation in tunnel with 90 ⁰ shaft.....	36
Figure 33- Standing pocket in 45 ⁰ shaft.....	38
Figure 34-Comparisson of critical velocities determined in the experiment with Kent's equation	39
Figure 35-Pocket reaching the tank, 60 ⁰ , 50l/s	40
Figure 36-Pocket standing in the shaft, 60 ⁰ , 55l/s.....	40
Figure 37-Pocket standing in the tunnel in 60 ⁰ shaft, F=1.4.....	41
Figure 38-Dimensionless velocities depending on slope of the shaft	43

Figure 39-Shape of air pocket depending on the shaft inclination.....	43
Figure 40 Threshold for continuous air return in the inclined shaft and beginning of air accumulation in the tunnel	44
Figure 41- Blowout monitoring at Holmaliåna (Utvik Gjerde, 2009)	45

Table list

Table 1-Test procedure.....	27
Table 2-Flow patterns types occurring in the shaft with slope 45 ⁰ and 60 ⁰	28
Table 3- Flow patterns in 45 ⁰ shaft	29
Table 4-Flow patterns in 60 ⁰ shaft	29
Table 5-Flow patterns occurring in 90 ⁰ shaft.....	31
Table 6-Flow pattern in 90 ⁰	32
Table 7 Discharge for beginning of air accumulation in the tunnel.....	35
Table 8-Determined values for critical velocity.....	37
Table 9-determined values for threshold flow velocities for continuous return	39
Table 10-determined values for clearing velocity.....	42
Table 11-Summary of determined dimensionless velocities.....	42

Symbols

A_p	-pocket head cross-section area
C_d	-drag coefficient
g	-earth gravitational acceleration
D	-conduit diameter
D_m	-model dimension
D_p	-prototype dimension
V_p	-pocket volume
L_p	-pocket length
F	-dimensionless flow number
F_c	-critical flow number
F_{return}	-threshold flow velocity for return
F_{clear}	-clearing velocity
F_D	-drag force
F_B	-buoyancy force
ρ_a	-air density
ρ_w	-water density
n	-dimensionless pocket volume
ρ_a	-air density
ρ_w	-water density
Q_w	-water discharge
Q_i	-water discharge
π	-Pi number
Re	- Reynolds number
S_0	-conduit slope
v	-superficial velocity
v_m	-velocity in the model
W	- Weber number
v_m	-velocity in the model
v_p	-velocity in the prototype
NTH	-Norsk Teknisk Høyskole
$\sin\theta$	-shaft inclination

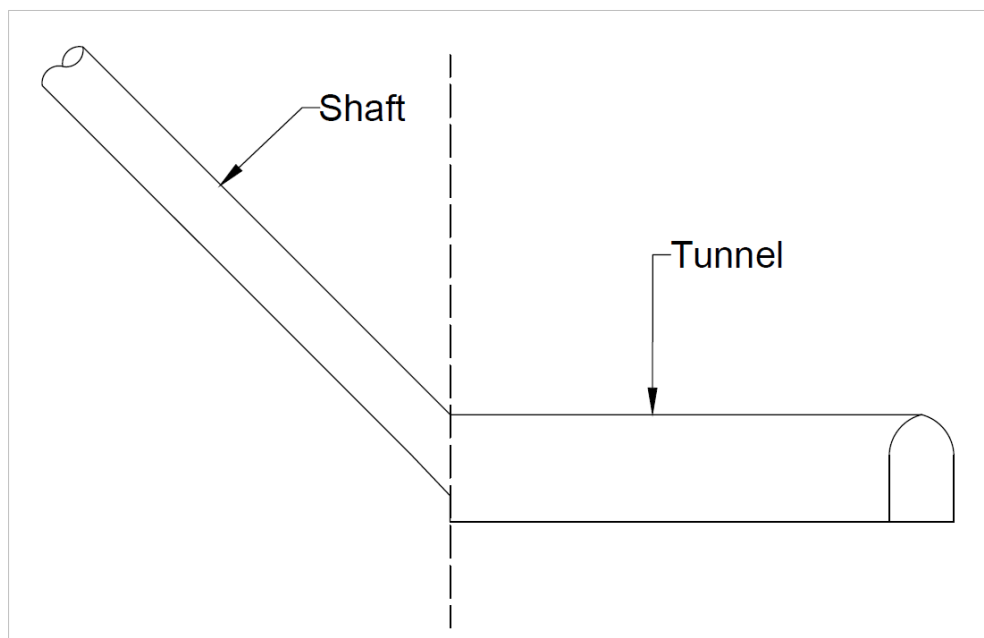
Terminology

- Froude scaled non-dimensional velocity, also known as the *Flow number*, can be defined as

$$F = \frac{v}{\sqrt{gD}}$$

where v is a superficial velocity which is a velocity the flow would have if only liquid phase was present. It is important not to confuse the flow number with Froude number, which is the ratio of liquid velocity and propagation of a wave in shallow water.

- *Flow regime* - intuitive description of the phase distribution along the pipe
- Term *bubble* is used to describe air bubble of any size which is not stationary and doesn't grow due to air accumulation.
- Term *pocket* is used to describe a larger volume of air in the model which is growing in size due to accumulation. The pocket is elongated and spread along the ceiling.
- Term *shaft* is used to describe the steep inclined circular part connecting the intake with the tunnel.
- Term *tunnel* is used to describe the part shaped like a horseshoe and mildly inclined.



1 Introduction



Figure 1-Outblow at Holmaliåna brook intake (Bekkeinntakskomiteen, 1986)

In Norwegian hydropower practice, it is common to construct additional intakes to collect the water from smaller streams in order to increase the production of a hydropower plant. Those brook intakes are usually built together with a small dam situated across the creek. From the intake, the water is conducted via a blasted or drilled shaft to the transport tunnel or a head race tunnel. Water entering the shaft can cause air entrainment into the tunnel system. This phenomenon, if not handled properly, can lead to problems like air accumulation resulting in head loss, supersaturation in downstream water or harmful blowouts. The issue of blowouts became more frequent in Norway as shafts became narrower when the building technology changed from blasting to drilling. The problem with blow-outs has also been reported in countries like USA, Switzerland, or Austria.

The phenomena considered in this thesis are confined to air and water flow in closed conduits. The mixed air-water flow in the pipes and tunnels can lead to hazardous situations. Notably, at brook intakes due to high velocities in the shafts the water may contain a large amount of trapped air which can then form air pockets in the tunnels. If the volume of the pocket is large enough to win against the drag force of the flow, the air pockets can be set in motion and lead to a powerful blowout.

Report of Bekkeinntakskomiteen, (1986), distinguishes small and large blowouts. The general aim is to avoid large blowouts which can be destructive. Based on the experiments of Berg (1986), the Bekkeinntakskomiteen prepared guidelines in order to avoid flow conditions which can lead to large blowouts. A desirable situation is when water flow in the conduit allows for the continuous return of air pockets of smaller size which cause no or little hazard.

1.1 Problem statement and methodological approach

Much of the existing research which covers the topic of air movement in closed sloping conduits focuses on conduits of smaller size and angles lower than 45° . Since brook intakes are usually designed with a slope 45° or more, it is crucial to observe the behavior of air in such conditions.

The overall goal of this thesis is to investigate the threshold flow for the continuous return of the air in steeply inclined shafts. Moreover, to conduct a study on air behavior and the flow patterns occurring in the shaft.

Due to its complexity, the process of air movement in closed sloping conduits is difficult to model with the use of numerical computations. The primary aim of the Master project was to design and build a physical model to study air-water flow and to set up a testing program for air return in the inclined shafts.

1.2 Structure of the Master thesis

Chapter 2 is dedicated to the theory of air movements in closed conduits. It presents and discusses some of the most relevant studies with regard to the topic. Chapter 3 deals with the design and the set-up of the model. Chapter 4 describes the laboratory experiment including test procedure, measured quantities, varying parameters, and resulting test data. Chapter 5 includes analysis of experimental data. Chapter 6 draws the conclusions and Chapter 7 gives recommendations for further research.

2 Theoretical background and literature overview

This chapter starts with an overview of the air-water two-phase flow theory and a discussion of the phenomena of air entrainment and air movement in closed water conduits. Further, different research on air transport is described. Finally, research studies examining the threshold velocity for continuous air return against the flow are reviewed.

2.1 Two-phase flow

Two-phase flow is a combined flow of two different phases. A phase is defined as a state of matter and can be liquid, gas or solid. Flow, where several phases occur simultaneously, is called a multiphase flow. Two-phase flow is the simplest case of multiphase flow. An example of a two-phase flow is an air-water flow where liquid and gas flow together. The flow is concurrent when air and water compounds move in the same direction. For situation when they move in opposite directions, the flow is termed counter-current.

2.1.1 Flow patterns in horizontal and vertical conduits

The fundamental difference between a single-phase flow and gas-liquid two-phase flow is the presence of flow pattern or flow regimes in two-phase flow i.e. the characteristic distribution of liquid and gas phases in the flow conduit. “Flow regimes determine the macroscopic behavior of two-phase flow” (Palsson, n.d.). Because of the complexity of air/water flow mechanism, first methods used to determine flow patterns in closed conduits were based on the empirical approach. A modern approach developed in the 1980s is called the mechanistic modeling. This method includes identification of the flow patterns occurring in the system and then mathematical modeling of the flow mechanisms behind the occurrence of the identified patterns. This combined theoretical and experimental approach gave a more detailed understanding of the two-phase flow phenomena. Two-phase flow patterns in the conduit depend on discharge magnitude of water and air as well as the conduit inclination. Different classifications of flow regimes can be found across the literature and researchers in the field have not yet reached an agreement on universal models that can be accepted for general flow situations.

Figure 2 illustrates regimes for horizontal flow in pipes, where the heavier liquid phase is most often located close to the conduit bottom.

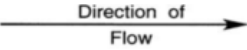
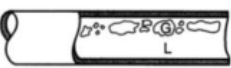



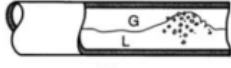
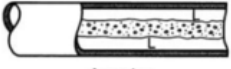

	
 Bubble	<p>The gas bubbles are dispersed in the liquid with a high concentration of bubbles in the upper half of the tube due to their buoyancy. Bubbles gather at the top of the pipe for low velocities. Bubbles become foam like at high velocities.</p>
 Plug	<p>Bubbles join and form larger gas plugs. This flow regime has liquid plugs that are separated by elongated gas bubbles. The plugs flow in the upper part of the pipe because of gravity effects.</p>
 Stratified	<p>The phases are completely separated with gas in the upper part and liquid in the lower part of the pipe. The gas goes to the top and the liquid to the bottom of the tube, separated by an undisturbed horizontal interface. Hence the liquid and gas are fully stratified in this regime. This type of flow can only occur at low velocity</p>
 Wavy	<p>Appears at higher velocities, compared to the stratified flow. Waves are formed at the phase boundaries, Waves travel in the direction of flow, The amplitude of the waves is notable and depends on the relative velocity of the two phases; however, their crests do not reach the top of the tube</p>
 Slug	<p>Waves in the flow reach the top of the pipe, closing the gas path at the top. The different momentum of the phases (because of velocity difference) results in sudden pressure changes when the path closes. Shocks and vibrations are experienced in the flow, and slug travels with a higher velocity than the average liquid velocity</p>
 Annular	<p>Once the interfacial shear of the high-velocity gas on the liquid film becomes dominant over gravity, the liquid is expelled from the center of the tube and flows as a thin film on the wall. Gas flows in the middle, possibly with liquid droplets traveling along it. The liquid film tends to be thicker at the bottom than at the top, because of gravity effects. This flow regime is particularly stable and is the desired flow pattern for two-phase pipe flows.</p>
 Disperse	<p>At very high gas velocities, all the liquid may be stripped from the wall and dispersed in the flow of gas in the pipe. The amount of liquid is much less in this case. Liquid velocity is very similar to the gas velocity.</p>

Figure 2-Flow regimes occurring in horizontal pipes, (Weisman, 1983), (Palsson, n.d.)

Characteristic regimes for flow in vertical pipes are summarized in Figure 3. In vertical conduits liquid tends to assemble on the walls of the conduit as stable or an unstable layer. The characteristic flow patterns will differ between upward and downward flows.

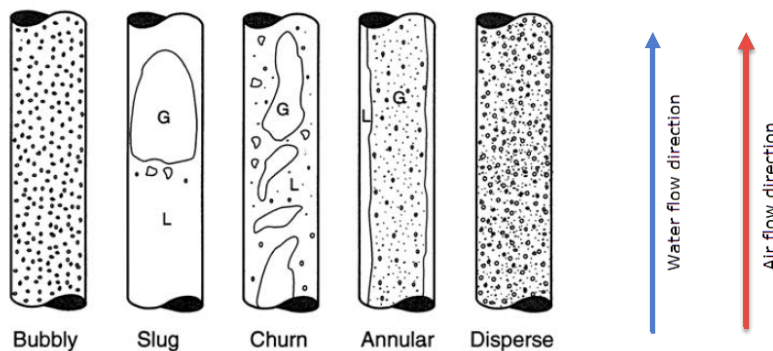


Figure 3 Flow regimes occurring in the vertical pipes (Weisman, 1983)

2.2 Air and water flow in downward-sloping pipes

2.2.1 Air entrainment

Air can be entrained into the system both in a dissolved form and as air bubbles traveling with the flow. In a typical brook intake water entering the shaft will have free surface flow until it reaches a level decided by the energy line and then change to full conduit flow. The air is entrained in the free surface flow and by a hydraulic jump, which occurs in the flow transition. The phenomenon is illustrated in Figure 4.

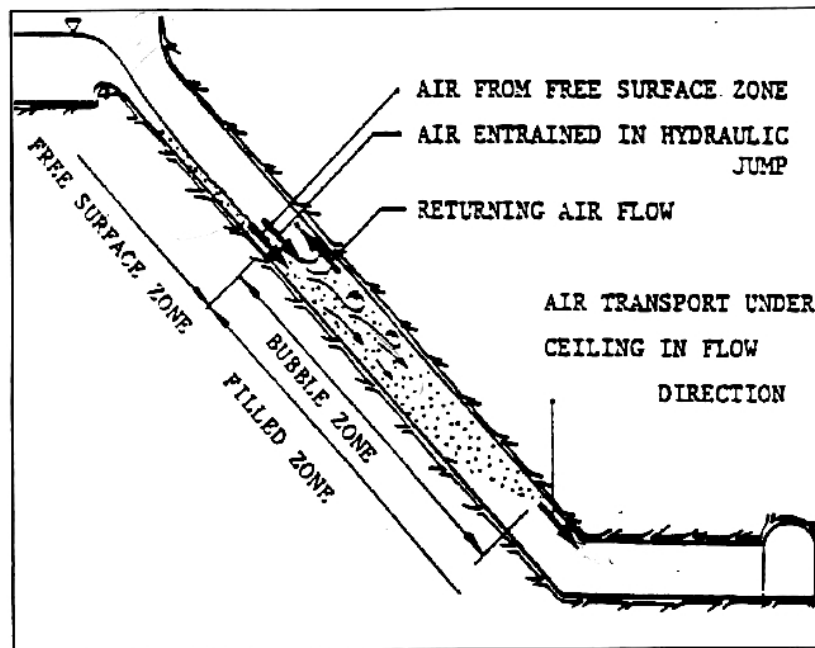


Figure 4 Air entrainment in Brook intake shaft (Berg, 1986)

The amount of the air entrained into the system depends on the flow velocity and the shaft characteristics i.e. geometry, roughness, and inclination. Entrained air is then transported down the conduit with the flow. For smaller discharges, the amount of air transported is limited by the flow capacity to transport the air. Air which will not be transported with the flow will return to the surface. For higher discharges, the air transport capacity of the flow increases. In this case the entrainment capacity of the hydraulic jump becomes the limiting factor for the amount of transported air. Bubbles traveling with the flow will tend to rise to the conduit ceiling. The section crossed by the bubble before reaching the ceiling is called a bubble zone. If the bubble zone reaches the bottom of the shaft and enters the tunnel, the bubbles will rise to the ceiling and may create air pocket(s). This pocket can either travel downstream the tunnel and cause problems like head loss or move upstream which may result in oscillations and damage to the intake.

2.2.2 Forces acting on an air bubble

Air, entrained into the system, depending on the flow conditions can either be transported with the flow or return to the surface. The transport capacity of air, in closed conduits, is governed by the relationship between water flow direction and buoyancy force direction. If the buoyant forces of the air pocket are larger than drag force of the flow, the air pocket may travel upstream. The scheme drawing representing the acting forces which was created by Falvey (1980) is reproduced in Figure 5.

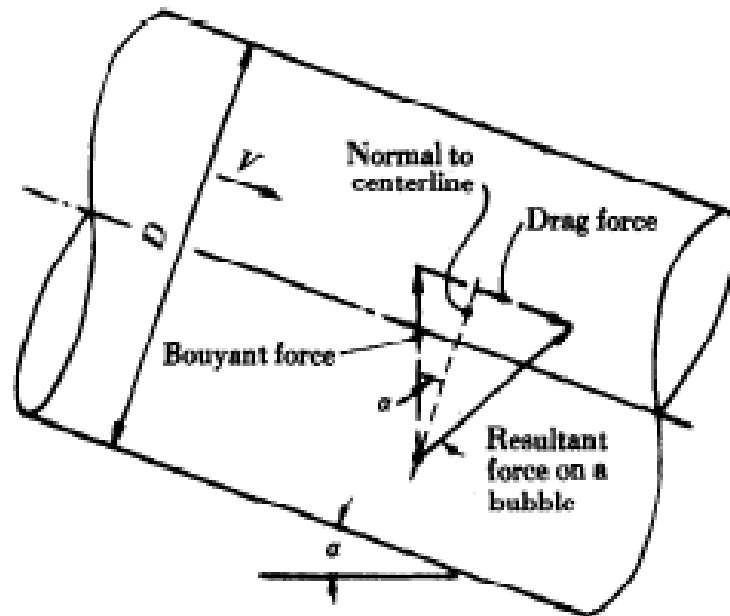


Figure 5 Forces acting on air bubble (Falvey, 1980)

The movement direction of the bubble being in equilibrium in the downward sloping conduit can be examined by comparing the relative magnitudes of the drag force and buoyancy. This situation can be approximately described by equation 1

$$C_d A_p \rho_w \frac{v^2}{2} = V_p (\rho_w - \rho_a) g S_0 \quad (1)$$

Where:

- C_d -drag coefficient
- v -mean flow velocity
- A_p -pocket head cross-section area
- V_p -pocket volume
- ρ_w -water density
- ρ_a -air density
- S_0 -conduit slope

Air density is much smaller than water density. Therefore it can be neglected. Equation 1 can be rearranged to:

$$\frac{v^2}{gL_p} = \frac{2S_0}{C_d} \quad (2)$$

Where: $L_p = V_p/A_p$ – air pocket length

Drag force and the shape of the bubble, cannot be determined numerically for a closed conduit flow situation. Important parameters for correlation between analytical results and experimental data need to be determined with use of techniques of dimensional analysis (Falvey, 1980). This topic is discussed in chapter 3.1.

For the assumption that the size of the pocket is dependent on the conduit diameter, further analysis leads to the conclusion that the velocity needed for air to move is a function of Froude, Reynolds and Weber number as well as pipe slope and pocket geometry.

$$\frac{v}{\sqrt{gD}} = f\left(S_0, n, \frac{L_p}{D}, Re, W\right) \quad (3)$$

Where: n - pocket volume/ $\frac{\pi D^3}{4}$
 D - conduit diameter
 Re - Reynolds number
 W - Weber number

Several authors (Kalinske & Bliss, 1943), (Falvey, 1980), (Pozos, et al., 2010) distinguishes the dimensionless flow rate which for a circular conduit with cross-section $A = \frac{\pi D^2}{4}$ is

$$\frac{Q_w^2}{gD^5} \quad (4)$$

Where: Q_w -water discharge

2.2.3 Formation of air pockets

In principle, air pockets will form if the air transport capacity is exceeded in conduit flows. In this situation, the detrained (ripped off) air will accumulate at the top of the conduit and form air pockets.

When the air transported through the shaft reaches the tunnel section the flow conditions change. Lower flow velocity and higher pressure in the tunnel causes the air bubbles to rise to the ceiling and accumulate. Figure 6 illustrates the return flow, occurring in the transition between the shaft and the tunnel, which leads to a local drop of pressure. Due to higher flow velocity, the pressure in the shaft is lower than in the tunnel. Air tends to travel towards the point with lower pressure. Hence, after reaching the tunnel ceiling air will most likely travel

in the direction of the shaft. If the flow in the shaft prevents the air pocket from traveling upstream, the pocket becomes stationary at the transition point until the conditions change (see Figure 7).

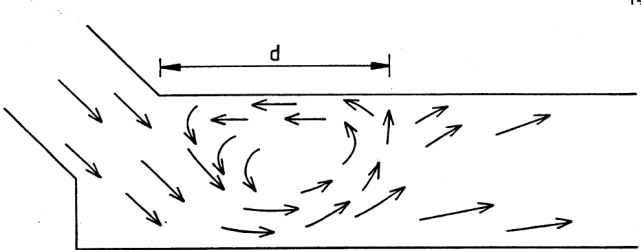


Figure 6 Return Flow (Berg, 1986)

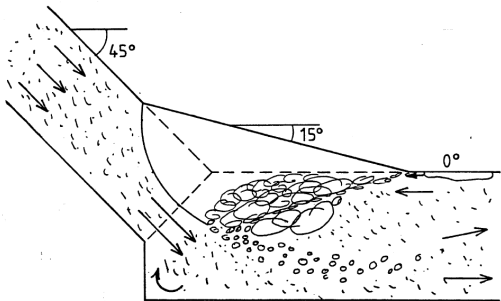


Figure 7 Air pocket (Berg, 1986)

Air pocket fills up a part of the conduit causing a change in the flow conditions. The conduit flow becomes constricted and water flowing under the pocket accelerates. Large velocity difference at the end of the pocket will lead to the formation of a hydraulic jump causing its erosion. Whether the pocket will grow depends on the amount of air returning along the tunnel ceiling. For situations with large water discharge, the air pocket can grow to a significant size before eventually returning through the shaft. When the discharge in the shaft decreases and the pocket is large enough to withstand the drag force of the flow, it may travel upstream. An blowout can occur when larger amounts of compressed air are released from the tunnel to the shaft. While travelling up the shaft, the air will expand and press the water out of the shaft causing an out blow which can be harmful to the intake structure. This situation occurs most often after a flood period when the water level at intakes is high but descending. (Berg, 1986) Formation of large air pockets in a conduit system is a common phenomenon occurring mainly because of bad design criteria which do not give enough consideration to the causes of air entrainment and related to this potential hazards and problems. (Pozos, et al., 2010). To avoid accumulation of air in larger volumes it is crucial to maintain a flow velocity for which the air can return continuously.

2.2.4 Air removal

An air pocket can be removed from an inclined conduit in a twofold manner:

1. Gradually by erosion caused by the hydraulic jump occurring at the end of the pocket.
2. By transport/removal of the whole pocket with the water flow.

Several terms were introduced with regard to air pockets removal mechanism. A term *critical or sweeping velocity* denotes the minimum velocity of the flow needed for an air bubble to move downstream in an inclined conduit. A term *clearing velocity* is used to define the minimum mean velocity needed to move the full air pocket to the bottom of the conduit (Yang & Liu, 2013). Both critical velocity and clearing velocity are functions of the pocket volume and geometry, Reynolds number, surface tension and pipe slope. In situations when the surface tension can be neglected, for a given conduit slope, velocity becomes proportional to:

$$(gD)^{1/2}$$

Where: D - conduit diameter

As the result of extensive debate on the topic of air movement in sloping pipes, it has been agreed to express the dimensionless velocity as a flow number, varying according to the pipe slope.

$$F = \frac{v}{\sqrt{gD}} = f(S_0) \quad (5)$$

Where: F -dimensionless flow number

v -superficial velocity

The equation 5 gives a convenient way to compare the results with the results from previous research. Knowledge of clearing velocity is crucial for the design of sewerage systems and water transport conduits to avoid head loss due to standing air pockets in the pipes.

2.3 Literature review

2.3.1 Previous studies on air transport

One of the first major studies on gas transport in downward sloping pipes was published in 1943 by Kalinske and Bliss. The authors distinguished different flow regimes occurring according to the existing flow conditions.

- For small discharges, they distinguished a blow back regime, where bubbles collide and occasionally blowback affecting the net air transport. In this case, the air transport is governed by the flow characteristics below the hydraulic jump.

- For higher discharges, a full gas transport regime was distinguished in which all the entrained air is being carried with the flow. Thus, the air transport becomes dependent on the conditions upstream from the hydraulic jump.
- Transitional flow regime at which stationary pockets can be observed in downward sloping conduits

Kalinske and Bliss determined the dimensionless flow rate needed for bubbles to be ripped off from an air pocket by the hydraulic jump occurring at its end at larger flow velocities. Based on the experiment performed for conduits of size 100 mm and 150 mm they proposed the following relation for downward sloping pipes.

$$\frac{Q_i^2}{gD^5} = \sqrt{\frac{\sin\theta}{0.71}} \quad (6)$$

$$\frac{v}{\sqrt{gD}} = \frac{4}{\pi} \sqrt{\frac{\sin\theta}{0.71}} = 1.51\sqrt{\sin\theta} \quad (7)$$

Kalinske and Bliss stated that to achieve a total removal of the air pocket the dimensionless flow needs to be significantly larger than the one required to start the transport of the air bubbles downstream.

Kent (1952) performed series of experiments on stationary pockets in downward sloping pipes covering the range between 15° and 60° with the use of 33 mm and 102 mm pipe. His focus was on determining the drag force in relation to air pockets geometry. Kent stated that the drag force coefficient becomes constant for pockets longer than 1.5 the size of conduit diameter D . As a result, Kent could estimate the buoyant force needed to balance the drag force for the pocket to become stationary. Based on the results coming from the experiments Kent proposed following relation for stable plug velocity:

$$F_c = \frac{v}{\sqrt{gD}} = 1.23\sqrt{\sin\theta} \quad (8)$$

Where: F_c -critical flow number

Later it was found that Kent made a mistake while graphically fitting relationship equation 8 to the result data. This was corrected by Wisner who made an improvement of the equation proposed by Kent and proposed the following relationship:

$$F_c = \frac{v}{\sqrt{gD}} = 0.55 + 0.5\sqrt{\sin\theta} \quad (9)$$

Gandberger (1957) investigated standing air pockets and pockets transport. For measurements, he mostly used pipes with a diameter 45 mm and with various inclinations covering the range between 5° and 90°. He concluded that pocket velocity becomes constant for pockets with non-dimensional pocket volume $n > 0.5$.

Falvey (1980) compiled previous research results for bubble movement in inclined conduits covering the angle range from 0° to 45° and presented results in an aggregate graph reproduced in Figure 8. The graph shows limits for the motion of both air pockets and air bubbles. Falvey defines the so-called slug flow region which is similar to the transition region presented by Kalinske and Bliss. Falvey predicts that for angles larger than 45° the limit for air pockets movement will decrease.

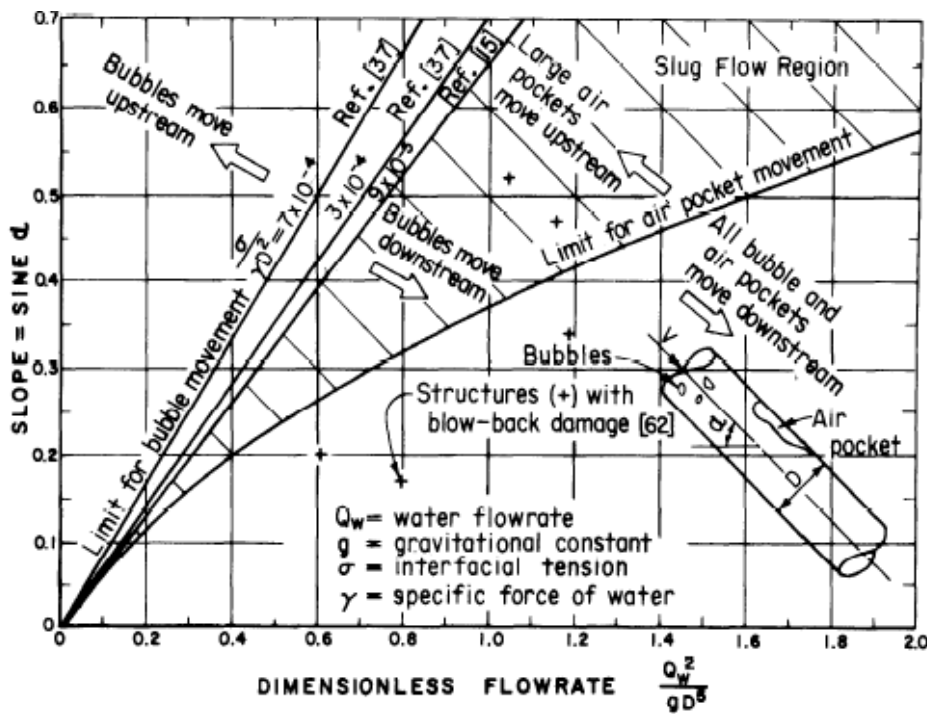


Figure 8- Air transport in closed conduit (Falvey, 1980)

Escarameia (2006) used for experiments a pipe with 150 mm diameter and proposed a relationship for critical velocity which is an extension of Kent's formula for angles below 15°.

$$F_c = \frac{v}{\sqrt{gD}} = 0.61 + 0.56\sqrt{\sin\theta} \quad (10)$$

Figure 9 shows the estimations for critical velocities depending on the conduit slope, developed by various authors.

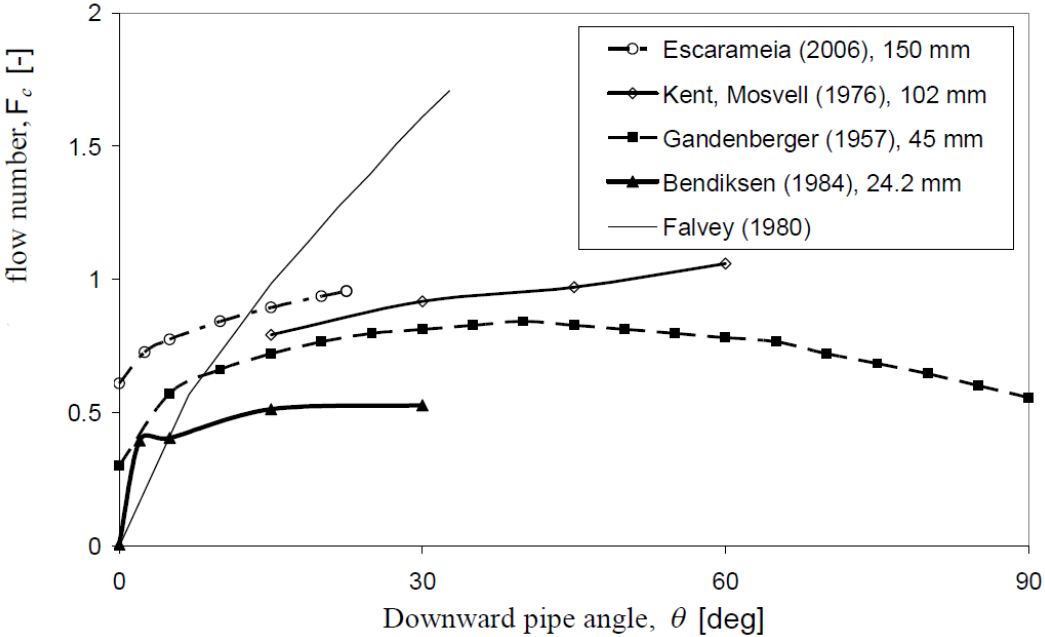


Figure 9 Critical flow numbers depending on pipe slope (Pothof, 2011)

Lubbers (2009) performed a series of experiments using pipes with diameters varying from 80 mm to 500 mm and inclinations ranging from 5° to 30° and 90° . Comparison of clearing velocities for pipes of different sizes led to a conclusion that this velocity becomes constant for pipes with diameter above 200 mm. Maximum clearing velocity is expected to occur for angles from 10° to 20° . Minimum clearing velocity is expected for a vertical pipe in contrast to the air transport which will be greatest in this case. The reason for this is the lack of an actual invert which helps the bubble to collide and accumulate into larger pockets. Furthermore, the drag force acting on the pocket will be higher due to the relatively larger surface of the pocket heads turned against the flow.

To “support the design of stormwater storage tunnels and bottom outlets of hydropower stations for the proper venting of pipes and tunnels” Pothof extended in 2009 the work of Lubbers .He derived an equation for clearing velocity depending on gas flow numbers based on an energy balance.

In 2010 Pozos combined the work of Kalinske and Robertson (1943) with work of Kent (1952) and proposed a simple relationship for the air movement which was later confirmed by experimental study.

$$\frac{Q_i^2}{gD^5} = S_0 \quad (11)$$

For a circular conduit:

$$\frac{v}{\sqrt{gD}} = \frac{4}{\pi} \sqrt{S_0} = 1.27 \sqrt{S_0} \quad (12)$$

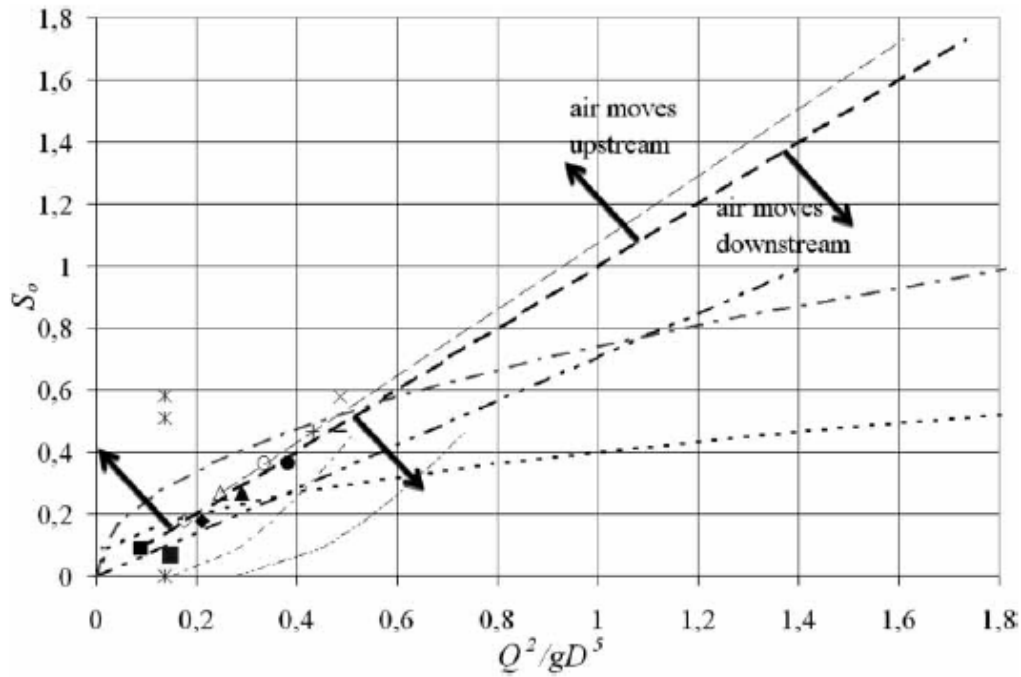


Figure 10 Air movement in downward-sloping pipes (Pozos, et al., 2010)

2.3.2 Previous studies on air blowouts in Brook intakes.

A series of research studies held at NTH tried to examine the threshold velocity for which no air can longer return against the flow in the shaft. The studies were based on the assumption that powerful blowouts may occur when air has no possibility to return up the shaft and is accumulated in the lower part of the shaft and tunnel resulting in the formation of large air pockets.

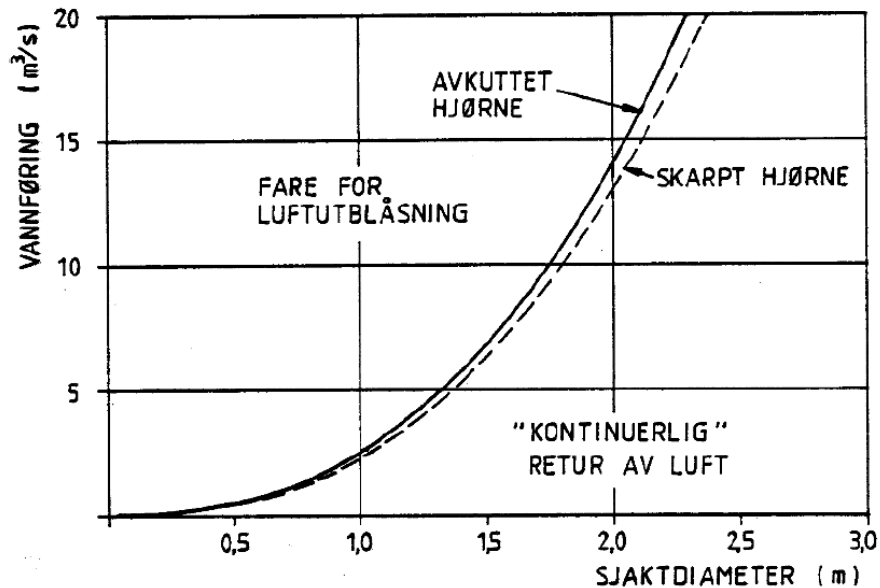


Figure 11 -Threshold velocity for continuous return of air (Berg, 1986)

Berg (1986) examined different forms of shaft to tunnel transition and looked at the shape of the standing air pockets. A model was created for the experiment representing the lower part of the shaft, transition part, and a horseshoe shaped tunnel (see Figure 13). The whole system was closed, and the hydraulic jump was created with the use of a sluice. The graph reproduced in Figure 13 summarizes results of Berg's experiment. The graph indicates the threshold discharge for continuous air return depending on the diameter of a circular shaft. Berg concluded that for a mildly shaped shaft to tunnel transitions threshold velocity occurs for the $F=1$ and for the sharply shaped transitions for the Flow number with a value of 0.95. Results were scaled according to the Froude's law. These results are believed to be valid when used for the design of structures for which the relationship between the cross-sections of the shaft and tunnel is up to 10:1. Berg found the flow conditions in the shaft were decisive for the air transport. Therefore, the results were scaled according to the shaft dimension. Results presented by Berg were used as the foundation for the Norwegian guidelines for design of brook intakes created by Bekkeinntakskomiteen (1986). These guidelines are still in use.

With some alternations, Berg's physical model was later used by Guttormsen (1986). The pipe with 59 mm diameter was connected to the main tunnel to model the velocity in the shaft with a different sloping angle. Results of this experiment are presented in Figure 12. Curve B represents the velocity above which the air cannot return, and the area between curve A and B represents the transition zone. As seen, the results for 45° inclined shafts are similar to what

Berg obtained in his experiment. Results presented in the figure come from a measurements with no extra air entrained via the shaft. All return of the air in the shaft stopped for $F=1$. For the measurement with air being entrained through the shaft, the value of Flow number was larger.

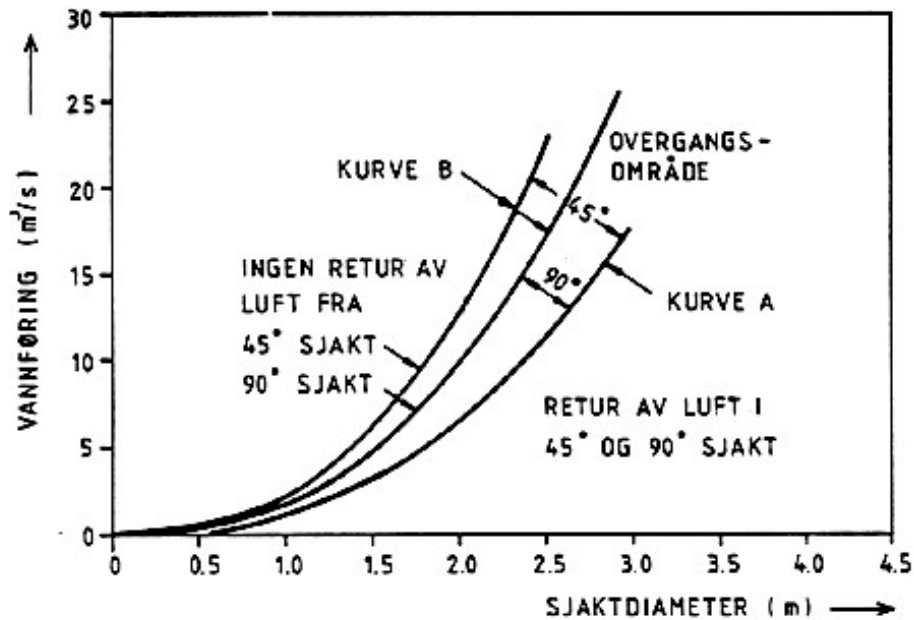


Figure 12-Results from a research with direct connection of shaft to the tunnel (Dahl & Guttormsen, 1986)

Research on the topic was continued by Gjerde in 2009, who used a similar model to the one used by Berg. In addition, by installing an open pool upstream, Gjerde in her model (see Figure 14) ensured the possibility to run the experiment both with an unsubmerged and submerged intake. Gjerde experiment showed that the air could still move from the tunnel upstream to the shaft for a flow with Flow Number value as large as 1.35. The amount of air returning for the same Flow Number was smaller for the free surface at intake than when it was submerged. This is probably due to the hydraulic jump and thus large turbulences occurring in a shaft with a free surface flow. For both situations with $F = 0.7$, the pockets became stationary in the shaft.

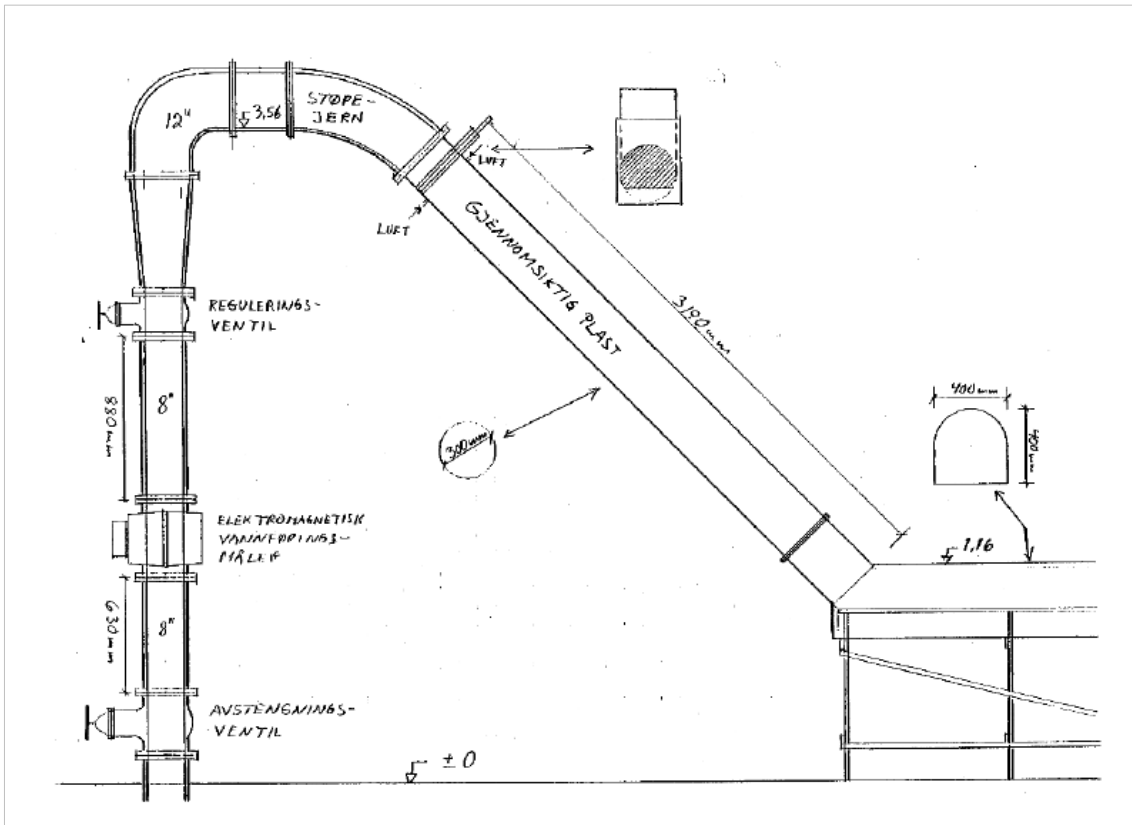


Figure 13 Experiment setup by Berg (Berg, 1986)

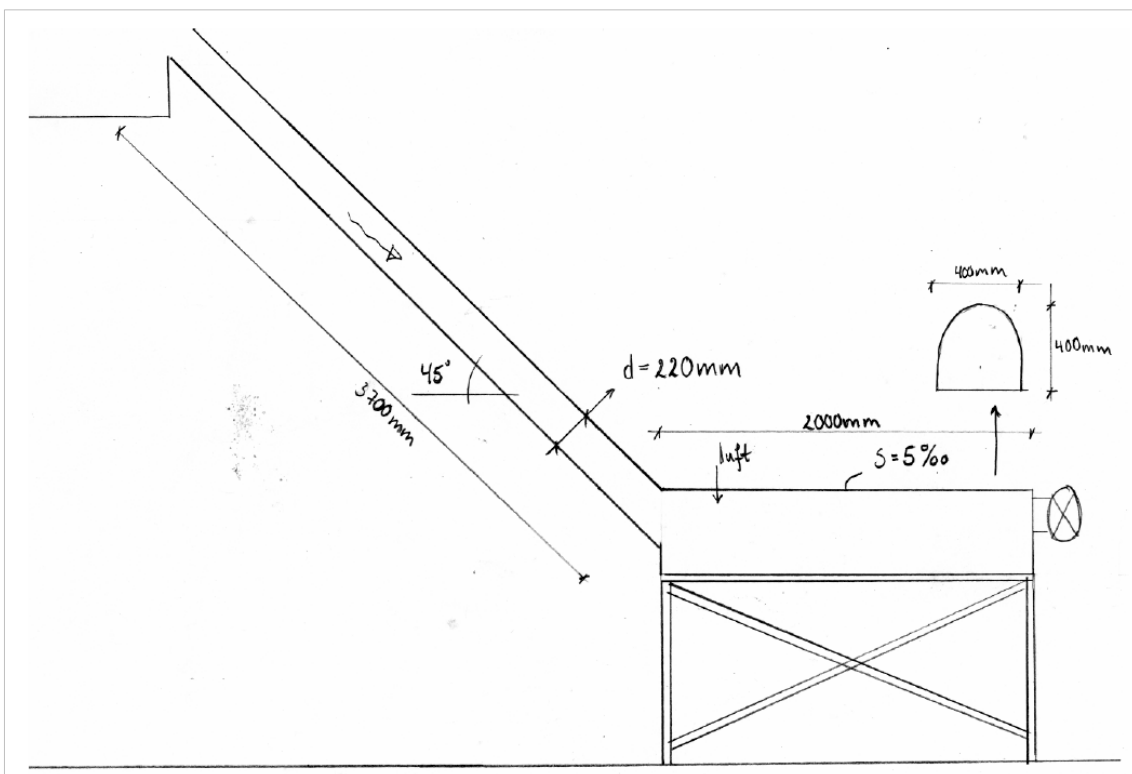


Figure 14-Experiment setup by Gjerde (Utvik Gjerde, 2009)

2.3.3 Air behavior in brook intake shaft

The majority of experiment results and derived relationships that are presented in chapter 2.3.1 were established with regard to the design of sewerage and water transporting systems. Results from these experiments reveal discrepancies. The main reasons for large scatter in obtained results are:

- different research methods that were applied,
- various materials and pipe sizes used to set up models,
- lack of actual measurements for larger conduit inclination.

The size of the conduit is expected to influence the results of the experiment for pipes with diameters below 200 mm. Most of the available research was performed with use of small pipes with diameter less than 150 mm, for which surface tension and viscosity influence the flow. Hence, scaling to larger dimensions of tunnels and shafts can lead to significant uncertainties.

All experiments were performed in smooth most often acrylic pipes. Therefore, roughness influence on air pockets was not captured in any of the experiments and most likely led to an underestimation of the actual critical velocity needed for air pocket propagation. Most of the tests were performed for slope angles smaller than 30° . Relationship equations were obtained by curve fitting to the results coming from these measurements. Values for the 45° angle and larger were usually obtained via extrapolation, and for this range, biggest scatter can be observed. Importantly, while Falvey's, Kalinske and Bliss', and Escarameia's equations show an increasing trend in non-dimensional velocity, Gandenberger's and Bendiksen's equations predict a decrease for angles larger than 45° .

When analysing standing pocket behavior on the transition from the tunnel to the shaft an uncritical use of relationships presented in chapter 2.3.1 could be misleading. This is due to change in geometry on the transition from shaft to the tunnel.

Flow needed to start the downward propagation of an air pocket will always be smaller than the flow needed to remove it from the conduit totally. Critical velocity could be regarded as threshold velocity for continuous air return. However, most research studies have proved the existence of a transition zone for which the critical velocity will represent the lower boundary and the threshold for no air to return will be the upper limit of the transition zone. It can therefore be assumed, that the magnitude of clearing velocity will be lower than the threshold

flow velocity for continuous air return and that the critical velocity will exceed the threshold
flow velocity for continuous air return: $F_{\text{clearing}} > F_{\text{continuous return}} > F_{\text{critical}}$.

3 Laboratory experiment

As stated previously, due to its complexity, the process of air movement in closed sloping conduits is difficult to model with the use of numerical computations. To study the phenomenon application of a physical model is thought to be the best solution. Experimental studies were carried out in order to understand the phenomenon of air movement in inclined conduits. A physical model was built in the NTH laboratory for this purpose.

Tests were performed for three model configurations with different slopes covering a range from 45° to 90°. The governing parameters investigated in this study include critical flow conditions, air accumulation mechanism, air-water mixture flow patterns, shape and behavior of the standing pocket.

3.1 Dimensional analysis

The dimensional analysis technique was used to help with the interpretation of experimental data. Major parameters influencing the outcome of the experiment were distinguished.

- Flow properties: *air density ρ_a , water density ρ_w , kinematic viscosity of air μ_a and water μ_w , surface tension γ , contact angle $\sin \phi$, flow velocity v , pocket length L_p*
- System parameters: *length of the inclined conduit L , conduit angle $\sin \theta$, conduit diameter D , roughness k_n ,*
- Physical constants: *gravitational acceleration g .*

Dimensional parameters were then grouped to create non-dimensional parameters. Finally, transport of an air pocket in a downward-sloping conduit can be expressed as function of the following dimensionless parameters:

$$\frac{v}{\sqrt{gD}} = f\left(S_0, n, \frac{L_p}{D}, Re, W\right) \quad (13)$$

Where:

n	-pocket volume/ $\frac{\pi D^3}{4}$
D	-conduit diameter
L_p	-pocket length
Re	-Reynolds number
W	-Weber number
S_0	-conduit inclination

3.2 Model scaling issues

Dynamic similarity is achieved when all non-dimensional parameters are the same in the model and in the prototype. This similarity, however, can not be obtained for a two-phase flow. When scaling dimensions with respect to Froude's law the Reynolds and Weber scaling laws cannot be fulfilled simultaneously. In order to minimize the scaling effects, it is crucial to secure a condition for which the influence of the viscous and surface tension forces is negligible.

The flow occurring in the model and the prototype has for most cases a Reynolds number Re exceeding the value 10^5 which is the value for which Re has an influence on the measurements. Zukowski (1966) stated that viscous and surface tension forces are of little significance for pipes with a diameter larger than 175 mm. For a situation when both viscous and surface tension forces can be neglected, angle S_0 in the model is the same as in the prototype and the air pocket geometry is modeled accurately regarding n , L_p/D . Consequently, the non-dimensional velocities in the model and the prototype are equal (see relationship 14) and then the model is correctly modeled according to the Froude's scaling law.

$$\frac{v_m}{\sqrt{gD_m}} = \frac{v_p}{\sqrt{gD_p}} \quad (14)$$

Where: v_m -velocity in the model
 D_m -model dimension
 v_p -velocity in the prototype
 D_p -prototype dimension

3.3 Design of the model

The model should represent a shaft connected to the tunnel. Due to space restriction, it was not possible to build a model of the entire shaft. Crucial for the experiment was modeling of flow conditions occurring in the lower part of the shaft and in the transition to the tunnel. Therefore, it has been decided to build a model representing only the bottom part of the shaft and a part of the tunnel. The shaft has been selected to be circular shaped and the tunnel part to be in a horseshoe shape.

In addition, following model criteria were considered:

- Model should include a possibility to carry out tests with the shaft at different inclinations.

- To avoid too much turbulence affecting the measurements, it is crucial to secure that the tunnel part of the model is long enough to prevent air being dragged out through the outflow.
- The ratio between the tunnel and shaft area should be large enough to secure a significant difference in flow velocities and to avoid extensive erosion of the pocket.
- The inclination of the tunnel similar to the one in the prototype should be secured to create favorable conditions for bubbles to return along the ceiling towards the shaft.
- Dimensions of the conduits should exceed 175 mm to avoid scaling effect.
- For the concern of visibility of the air pockets use of transparent material is needed.

3.3.1 Hydraulic jump in the shaft

In his experiment Berg (1986) created an artificial hydraulic jump with a use of a sluice. Gonzales and Pozos (2010) found that the distance from the jump must be at least 10 times larger than the diameter of the conduit for the transport not to be influenced by the turbulence effect caused by the hydraulic jump. The model ought to represent the lower part of the tunnel. In a prototype, the level at which the hydraulic jump is established is governed by the energy line in the system. Brook intakes are usually long, and it is possible to assume that the distance from the hydraulic jump will be greater than the length/diameter ratio estimated by Pozos. This will say that the hydraulic jump doesn't influence the flow at the bottom of the shaft. It was decided to set up a model in which the hydraulic jump would not occur.

3.3.2 Air entrainment to the model

The process of air entrainment is complex and difficult to model. To know the exact amount of air in the system, it is necessary to prevent air from entering the system from upstream. The intake should be submerged, and no vortexes should occur. For experimental purposes, the amount of air should be known, and the volume ratio between air and water should be constant. This can be achieved by the use of an air compressor for conditions where no air is entrained through the intake. Berg, (1986) states that the optimal conditions resembling those at the bottom of the shaft are created by providing air in a ratio of 1.3 percent of the water discharge. It was decided to accept this assumption. Air accumulating in the bottom of the shaft can have its source either from air entrained upstream or from air entrained at another brook intake and then transported with the flow through the tunnel systems. To model this, air entrainment in the model should be possible either from upstream into the shaft or directly into the tunnel.

In order to avoid the difficulty of removing the air returning up the shaft, it was decided to use an open tank as intake.

3.4 Testing facility and instrumentation description

The test facility was designed to operate as an open water circuit connected to the primary laboratory water circuit. NTH laboratory provides a maximum head of 7 m of water coming from a pool situated in the upper part of the building. Water was transported by steel pipes to an open tank with dimensions 110 cm x 90 cm x 70 cm that was placed at elevation 3.7 m (see Figure 19). Water from the tank was directed through the model and back to a sump connected with a pool placed in the underground of the laboratory. On return, water was pumped up to the upper pool.

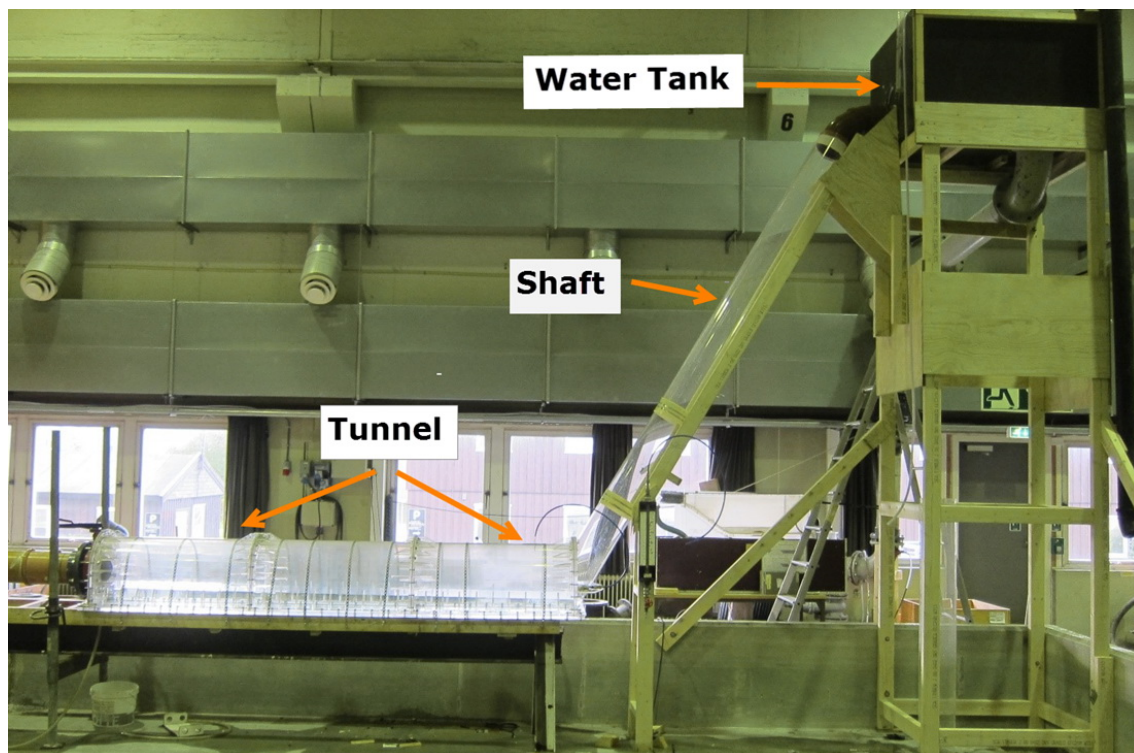


Figure 15- Brook intake model with the 60° shaft..

3.4.1 Model and instrumentation

Outflow from the tank was connected to the shaft pipe with a prefabricated PVC elbow pipe. Depending on the rig setup the angle of this connection would vary. The shaft was made from a transparent acrylic pipe with an inner diameter 210 mm and wall thickness 5 mm. The tunnel part was made from acrylic parts that were reinforced with ribs and screwed together. The tunnel was 3 m long had an inclination of 0.5% and was horseshoe shaped with

an equal height and width of 40 cm. Mesh was placed in the tank to prevent turbulences caused by the water coming from the bottom (see Figure 16).

Water discharge was regulated with a gate valve (see Figure 19). Water elevation in the model was regulated with the use of a butterfly valve placed at the outflow from the tunnel part (see Figure 17). Maximum head achieved in the model was 3 m. Maximum discharge used during measurements was 70 l/s.

Air was provided to the model either directly to the tunnel by a vent placed in the tunnel roof or to the shaft with use of a hose (see Figure 16). Air was distributed with the use of a compressor. The maximum amount of air that could be provided was 55 l/min.

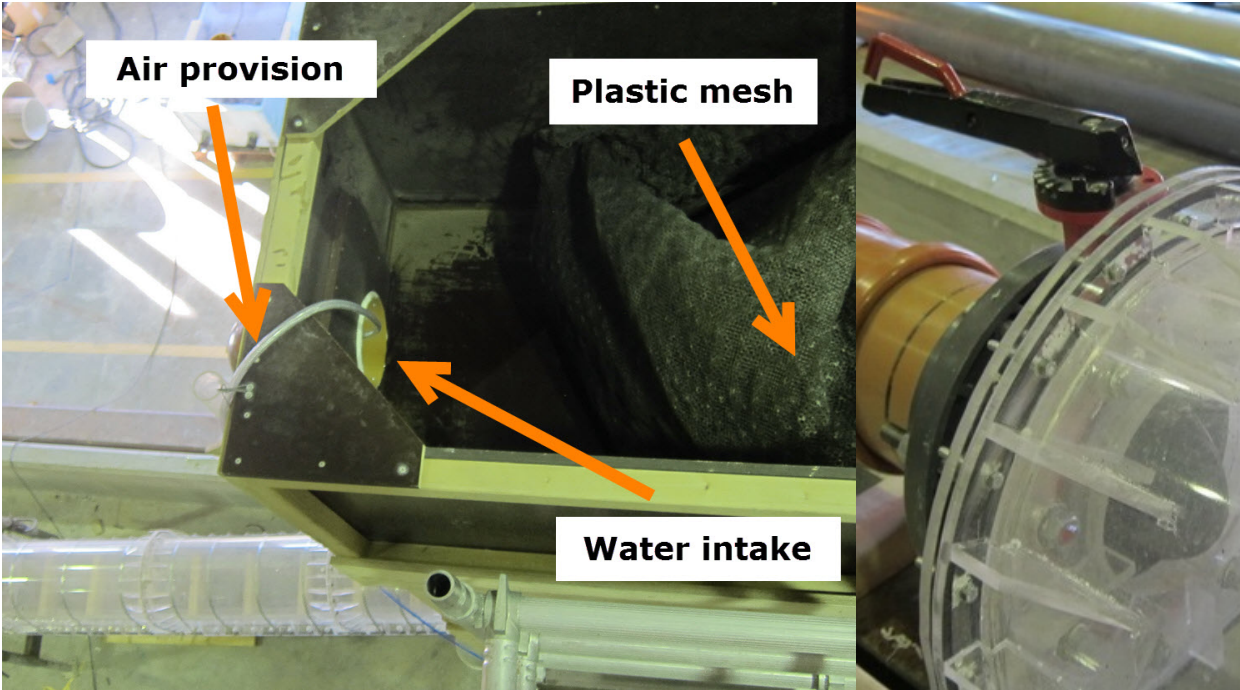


Figure 16- Water tank, view from above.

Figure 17- Outflow regulation with a butterfly valve

The model allowed for three different settings with different shaft slopes. For angle 45° and 60° a transition part was built from shaft to the tunnel. For 90° the shaft was connected directly to the tunnel top. Depending on the inclination the shaft had following length:

Shaft inclination (degree)	Shaft length (cm)
45	240
60	190
90	160

A sketch representing the model in different setups is presented in Figure 18.

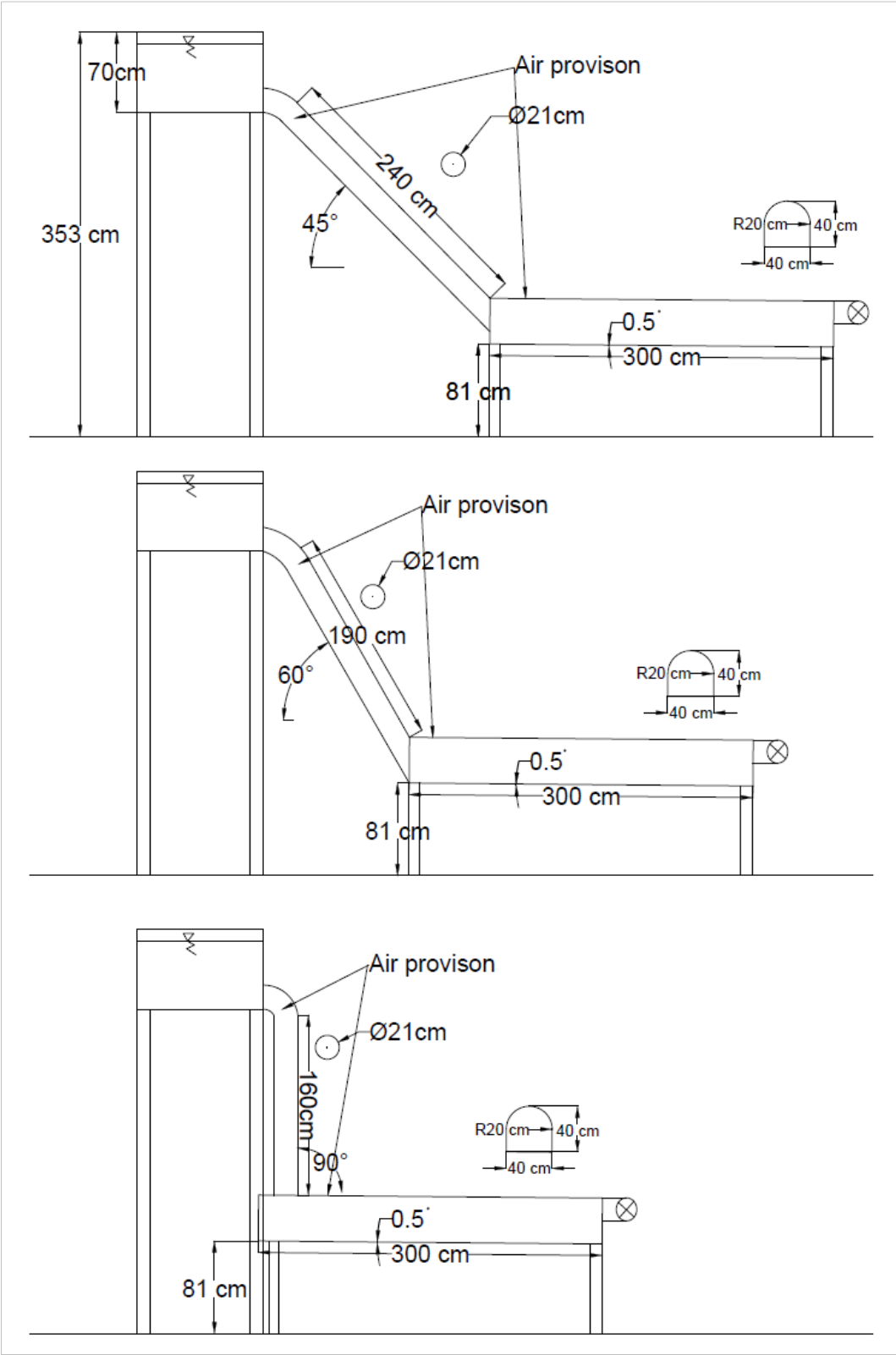


Figure 18- Model setup for 45, 60, 90 degrees.

The following simple devices were used for measurements and observations during the experiment:

1. Electro-Magnetic Flow Meter ABB Kent-Taylor MagMaster used to measure water discharge provided to the model (see Figure 19)
2. Rotameter type Metric 18A- measuring the air discharge provided to the model (see Figure 20)
3. Video camera-capture of moving bubbles and pockets
4. Photo camera documentation of the experiment

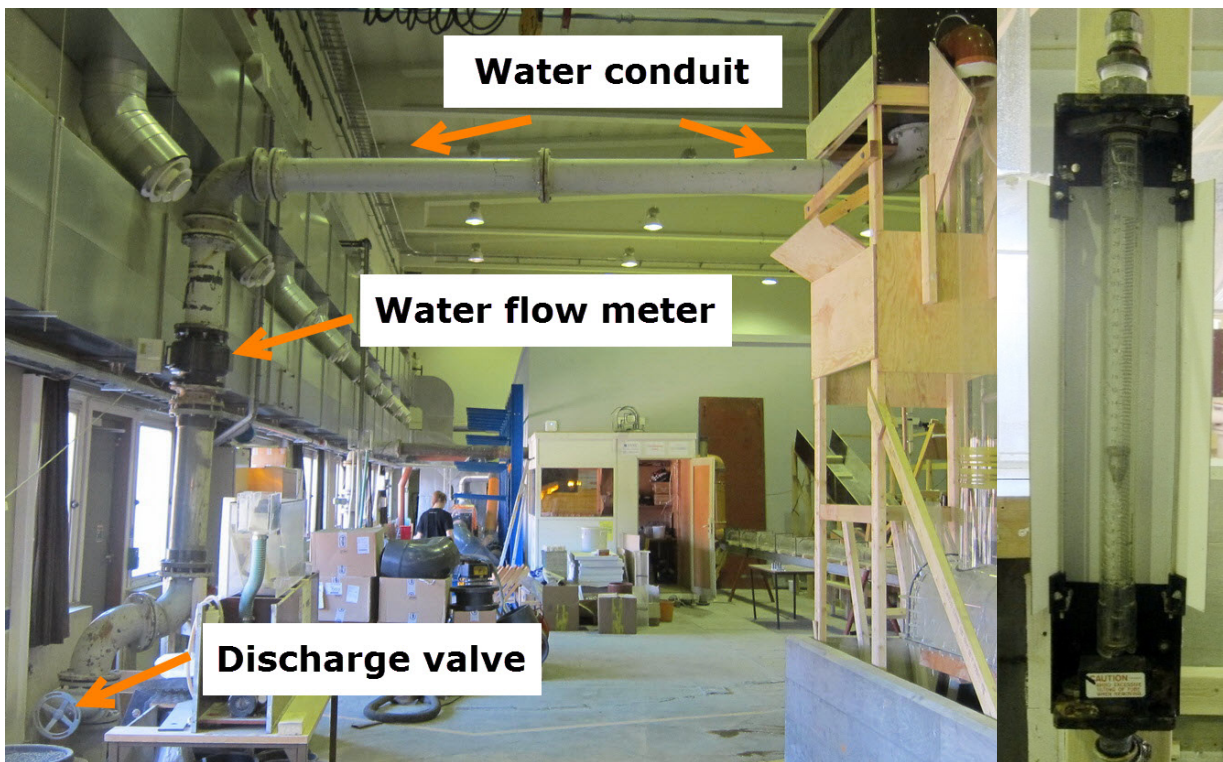


Figure 19- Water provision to the model



Figure 20 Air flow meter

3.5 Experiment procedure

The purpose of the experiment was to examine the behavior of air pocket in a downward sloping conduit for various angles. Detailed investigation of the flow patterns in the shaft and flow conditions in the tunnel were performed. The following values were determined based on the results of the experiment:

- Critical velocity,
- Clearing velocity,
- Threshold flow for continuous air return.

3.5.1 Experiment configurations

Shaft inclination

The model setup allowed for a change of inclination of the shaft pipe. Change of inclination resulted in a change of the shaft pipe length. The model could be used with shaft sloping 45°, 60° and 90°.

Water discharge

Measurements were performed for different discharges. To avoid scaling effects due to viscous forces, the Re number had to be larger than 10^5 . The smallest discharge securing this requirement was calculated to be 17 l/s. The experiment was performed starting from 20l/s to the highest discharge of interest. It was decided to perform measurements with discharge increments of 5 l/s up to maximum discharge 70 l/s. Smaller increments were used when determining characteristic velocities.

Air volume

During the experiment, various amounts of the air were provided to the model. Air was added first to the tunnel then to the top of the shaft in the amounts stated below:

- The smallest amount of air resulting in air return of any kind.
- Air volume equal to 1.3% of the water discharge.

When a standing pocket occurred, a larger volume of air was provided to check whether the pocket will be influenced.

3.5.2 Test procedure

Prior to each measurement, a constant water head in the upstream tank had to be established. The main valve placed on the inflow pipe to the water tank was used to regulate the discharge.

The valve placed at the outflow pipe from the model was used to establish the water level in the tank to be high enough to avoid air entering through the intake. It was necessary to wait for a certain amount of time for the water elevation to be stable.

The measurement procedure included observations and measurements of the following processes and patterns:

Table 1-Test procedure


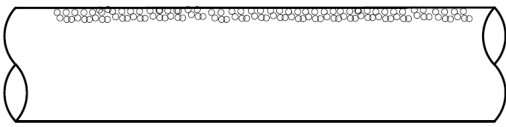
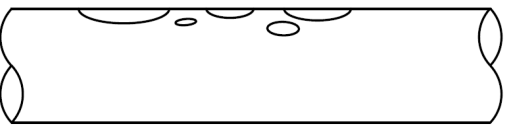
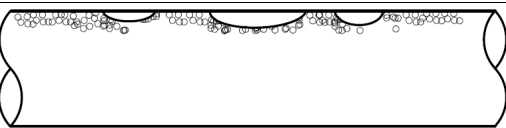
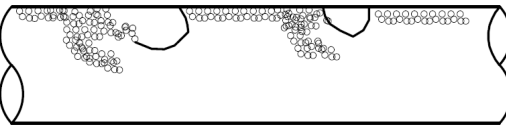
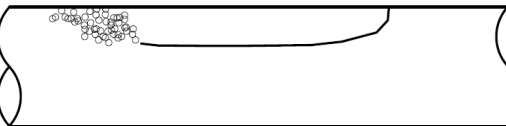
Observation/measurement	Information used for
Flow patterns in the shaft	
Flow patterns were assessed visually. The changing model configurations during the assessment were conduit inclination, discharge magnitude, volume of provided air and the point of air injection.	→ Study of flow conditions in the shaft → Study of conditions leading to blowout
Frequency of return	
The number of returning bubbles/pockets was counted for a time interval of 60 seconds. The changing model configurations during the assessment were conduit inclination, discharge magnitude and the point of air injection. During tests, the ratio of volume of provided air to water discharge was kept constant at 1.3%.	→ Relation between frequency of return and point of air entrainment (shaft, tunnel) → Relation between frequency of return and flow regime
Study of flow conditions in the tunnel	
Thickness of the pocket in the tunnel and the length of the bubble zone was measured for varying discharge and constant air to water ratio. In, addition flow regimes in the tunnel were observed, and beginning of the air accumulation registered. Video capture and photographs were used for measurements.	→ Study on flow conditions and air accumulation in the tunnel
Observations on air behavior:	
The observations were carried out visually. The following important characteristics of air behavior were registered: <ul style="list-style-type: none"> • Starting conditions for occurrence of stationary pockets in the shaft, • Flow conditions at which the air pocket stopped expanding to the shaft 	→ Critical velocity → Clearing velocity → Threshold flow for continuous return

4 Test results and observations

4.1 Flow patterns observed in the shaft

Flow patterns were observed for discharge varying within the range 20 l/s - 60 l/s and for shafts with slopes of 45°, 60° and 90° degrees. Flow patterns in the shaft changed depending on the water discharge, the amount and the point of air entrainment. Detailed observations for different air and water discharge setups gave a basis for distinguishing the key flow patterns occurring in the shaft. Table 2 gives a description of visual assessment of the observed flow patterns for a shaft with slopes of 45° and 60° degree and Table 5 for 90°.

Table 2-Flow patterns types occurring in the shaft with slope 45° and 60°

Type	Direction of air movement 	Description
1		Tiny bubbles accumulate at the ceiling but do not merge. This bubble swarm moves upstream along the ceiling.
2		Air travels upstream in form of bubbles of small or medium size. While going upstream, the bubbles erode.
3		Bubble swarm travels along the ceiling upstream. Larger bubbles move in-between the bubble swarm but with higher velocity.
4		Bubble Swarm is stationary or moving downstream. In some cases when the amount of air and flow turbulence is high, the air becomes dispersed over the whole pipe, and the flow turns into foam. Larger bubbles move upstream along the ceiling. Advancing bubble erode violently and close at a certain point leaving a whirl behind. The frequency of return is high. Bubbles travel relatively fast.
5		Air travels only as large pockets propagating slowly upstream. Anything else is carried by the flow downstream.

Shafts inclined 45° and 60°

Table 3 and Table 4 present the flow regime occurrence depending on the water and air discharge. Term *normal air* relates to the measurement when the air was provided in the ratio 1.3 percent of water discharge. Term *minimum air* relates to the measurements when the air was provided in the smallest amount allowing for return of any type.

Table 3- Flow patterns in 45° shaft

Discharge l/s	Flow pattern type			
	Air minimum		Air normal	
	Tunnel	Shaft	Tunnel	Shaft
20	1	x	3	x
25	2	2	3	3
30	3	2	4	3
35	4	2	5	4
40	5	4	5	4
45	5	5	5	5
50	5	5	5	5
55	5	5	5	5
60	5	5	5	5

Table 4-Flow patterns in 60° shaft

Discharge l/s	Flow pattern type			
	Air minimum		Air normal	
	Tunnel	Shaft	Tunnel	Shaft
20	2	x	3	x
30	3	1	4	3
35	3	3	5	4
40	4	3	5	4
45	5	3	5	5
50	5	4	5	5
55	5	4	5	5
60	5	5	5	5

*x-no measurement

Results presented in Table 3 and Table 4 indicate that for air introduced in the shaft, pockets occur in the shaft at higher discharges compared to the situation when the air is introduced directly to the tunnel. The results also show that amount of entrained air have an influence on the formation of the pockets. With more air entrained, pockets occur at lower discharges. The occurrence of pockets starts right after the beginning of air accumulation in the tunnel.

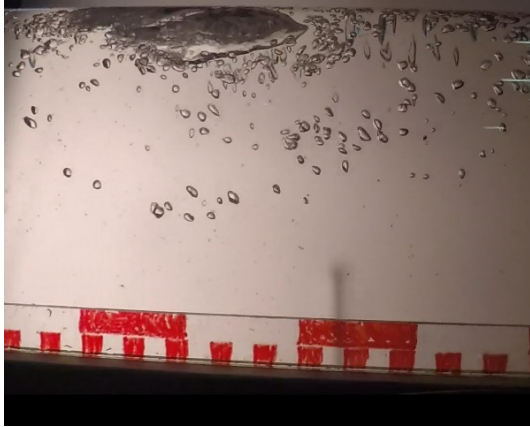


Figure 21-Type 3 flow regime, 45^o minimum air, 30l/s



Figure 22-Type 4 regime, 45^o, 1.3% air, 30l/s, bubble is closing

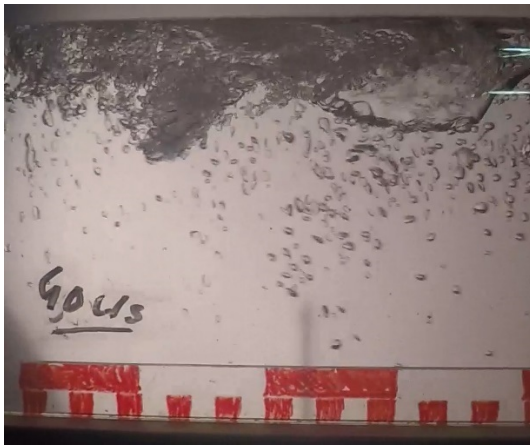


Figure 23-Type 4 regime, 45^o, minimum air, 40l/s

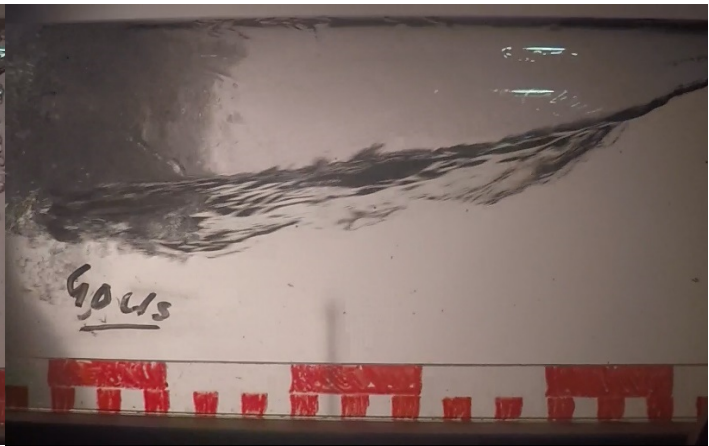


Figure 24-Type 5 regime, 45^o, 1.3% air, 40l/s

Comparing regime 4 and 5 it was observed that the air bubble in regime 4 would decrease in size faster due to erosion and turbulences created behind the advancing bubble, leading to a point where the bubble would close (see Figure 23 and Figure 24). The erosion of a pocket happened much slower and in a more gentle way. A pocket reaching the intake would still be of significant size.

Vertical shaft

Different flow regimes were observed for the model setup with vertical shaft (90°) due to lack of a ceiling allowing for air accumulation. Despite that majority of theoretical flow regimes in vertical conduits were identified for concurrent flow conditions the observed patterns for counter-current flows are similar to the ones described in the theory (see Figure 3).

Table 5-Flow patterns occurring in 90° shaft

	Flow pattern:			Description:
	Type 6	Type 7	Type 8	
Water flow direction ↓				<p>Type 6-Air returning from the tunnel to the shaft travels upstream in form of many bubbles which disappear fast due to erosion- can be compared with bubbly flow</p> <p>Type 7- Air travels upstream in form of a large pocket sticking to the pipe wall- can be compared with slug flow</p> <p>Type 8-When air is entrained to the shaft, the flow carries all air downstream in form of dispersed bubbles. With higher air discharges the flow turns into a white foam. No air travels against the flow.- can be compared with dispersed flow</p>

Analysis of the results for the vertical shaft suggest that generation of pockets starts at lower discharges than in the 45° and 60° inclined shafts. Table 6 reveals that the occurrence of pockets started for discharge => 30l/s regardless of the point of air provision.

Figure 25 illustrates a flow pattern type 7 that is similar to a slug flow regime.

Flow pattern type 8 having the characteristics of dispersed flow was occurring only when normal amount of air (ratio 1.3%), was provided to the shaft. For this flow regime, the air did not return up the shaft and was instead was accumulated in the tunnel. If the air provision was reduced, larger pocket would start traveling upstream. It is believed that in a full-scale design this mechanism could lead to a violent blowout.

Table 6-Flow pattern in 90°

Discharge l/s	Flow pattern type			
	Air minimum		Air normal	
	Tunnel	Shaft	Tunnel	Shaft
20	6	6	6	6
25	6	6	6	6
30	7	7	7	8
35	7	7	7	8
40	7	7	7	8
45	7	7	7	8
50	8	8	8	7

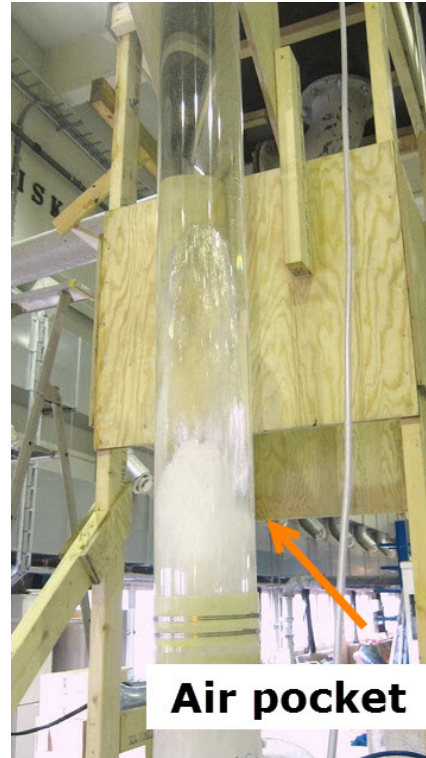


Figure 25 Pocket propagation in vertical shaft (Flow pattern 7)

4.2 Frequency of air return

The number of bubbles/pockets returning from the tunnel to the shaft was counted for a time interval of 60 seconds. The changing model configurations during assessment were conduit inclination, discharge magnitude and the point of air injection.

For equal water discharge in the model, two measurements were done. Firstly, with air provided to the tunnel and then to the shaft, both in an amount equal to 1.3% of the water discharge. Pockets expanding from the tunnel to the shaft that didn't split were counted as no return. Use of a constant air to water ratio allowed for comparison between the magnitudes of air return frequency depending on point of air provision in the model. The measurements of air return frequency dependent on point of air provision, for different inclinations are plotted in Figure 26, Figure 27 and the Figure 28. The experiment yielded the following major observations:

- The frequency of return varied depending on water discharge and the point of air provision. Behavior of air in 45° and 60° shafts was similar. For the vertical shaft, the results were different.

- For all inclinations, the frequency of returning bubbles would decrease with higher discharge while the size of the bubbles traveling upstream would rise.
- Measurements indicated that for the same discharge, frequency of air return was higher for situation of air introduced to the shaft until the 0 frequency was reached.
- For inclination 45⁰ and 60⁰ frequency of air return diminish to 0 for discharges higher than 50 l/s both for air introduced to shaft and tunnel. For inclination 60⁰ the 0 frequency was reached at slightly lower discharges than for 45⁰ shaft.
- For a discharge at which air introduced to the tunnel stops returning air entrained to the shaft can still return.
- Possibility for accumulation of larger volumes ergo larger blowouts is higher when the air comes from the tunnel side.

As stated above the measurements indicated that in general for the same discharge, frequency of air return was higher for situation of air introduced to the shaft than to the tunnel. The experiment for the 45⁰ inclined shaft (see Figure 26) revealed however, that for discharges lower than 35 l/s the opposite occurs i.e. when air was introduced to the shaft the frequency of return was lower compared to the situation when air was introduced to the tunnel. This is caused by the limited transport capacity of the flow in the shaft. For higher discharges, all air entrained to the shaft was transported to the tunnel. The decrease in frequency is noted for discharge higher than 30l/s for air introduced to the tunnel (change to flow regime 5- occurrence of pockets) and discharge higher than 35l/s for air introduced to the shaft (change to flow regime 4).

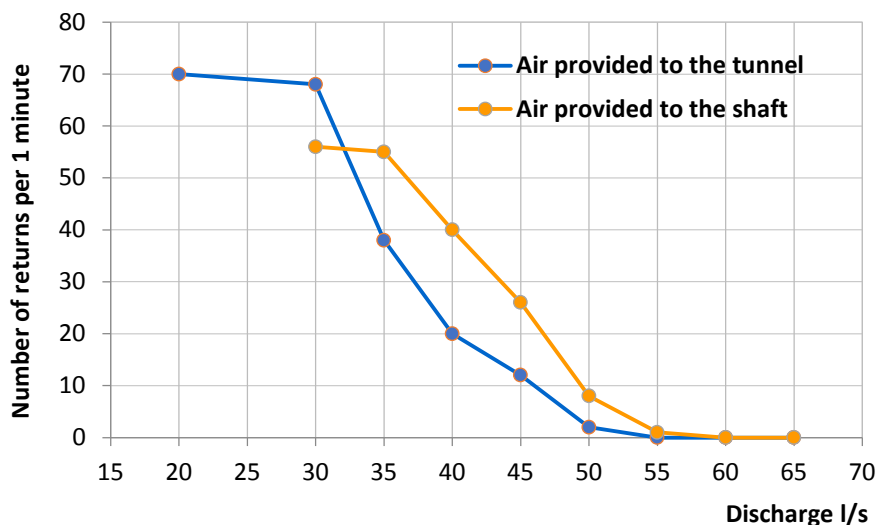


Figure 26-Air return frequency in 45⁰ shaft

Measurements performed for the 60° shaft are presented in Figure 27. For discharge lower than 25l/s air provided to the shaft didn't reach the tunnel, hence no return was recorded. Results show that for discharge 45 l/s and higher the air behavior is almost independent of air provision point. The reason for a sudden decrease in frequency (observed from 40 l/s to 45 l/s) for air entrained to the shaft can be explained with the change in flow regimes and occurrence of pockets. When compared to the results from the 45° shaft it is visible that the frequency of return for 50 l/s was lower, this will say that larger pockets occurred faster in the 60° shaft.

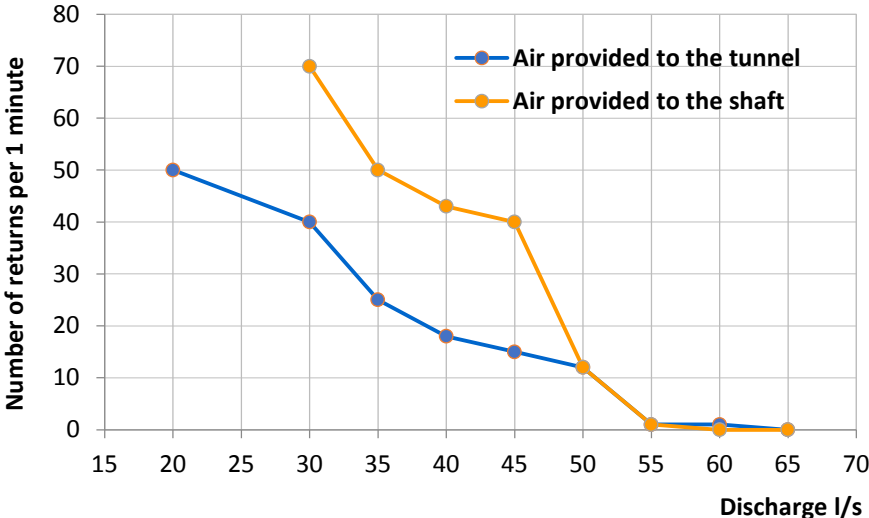


Figure 27-Air return frequency in 60° shaft

For the vertical shaft, air return frequency values for air entrained into tunnel are plotted in Figure 28. When air was entrained to the shaft it was not possible to measure the return, because air dispersed in the shaft prevented from any observations. Compared to results from 45° and 60° shafts it is visible that frequency values are smaller and reach the 0 value at lower discharge. This indicates that the returning pockets will be larger and the potential blowouts more violent (see Figure 28).

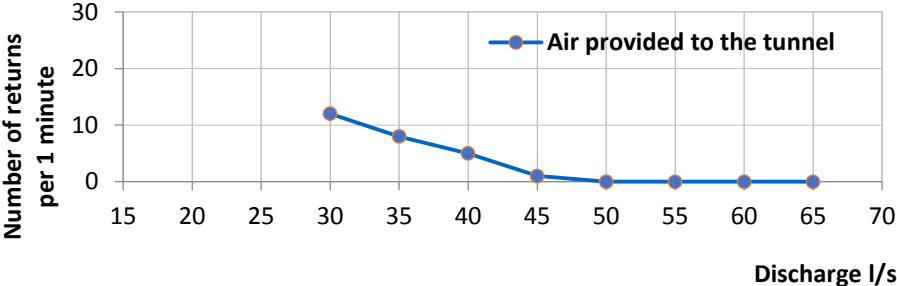


Figure 28-Air return frequency in 90° shaft

4.3 Observations in the tunnel

Additional observations of the air-water flow were carried out in the tunnel. Depending on the discharge, different flow regimes were observed. The water discharge (Flow number) in the model needed to start air accumulation in the tunnel was determined. Observations of shape and location of air pocket in the conduit were made.

4.3.1 Flow regimes occurring in the tunnel

Different flow patterns were observed in the tunnel depending on the water discharge and the different amount of air provided. The occurring flow regimes corresponded to the ones described in chapter 2.1.1 “Flow patterns in horizontal and vertical conduits”.

For lower discharges, the flow would be stratified. In the setup with the 45° shaft at 35 l/s discharge, when a larger volume of air was accumulated in the tunnel, the flow regime would change to wavy. Afterwards, the wave oscillating in the tunnel would increase its amplitude until reaching the top of the tunnel. This would create a pressured pocket between the subsequent wave crests. The force of the traveling wave would increase and the regime would resemble the slug flow. The wave traveling upstream the tunnel would often push the standing pocket into the shaft. The traveling wave is believed to have a potential to trigger a blowout and to create oscillations in the system. This situation was never observed in the setup with a 60° shaft. The wavy regime was neither observed in the setup with the 90° shaft.

4.3.2 Air accumulation

Beginning of air accumulation in the tunnel was observed for the following discharges:

Table 7 Discharge for beginning of air accumulation in the tunnel

Shaft angle [degree]	Discharge [l/s]	Flow number $F = \frac{v}{\sqrt{gD}}$
45	35	0.7
60	35	0.7
90	30	0.6

The air pockets had elongated shape. Two situations could be distinguished.

- Air pocket starting in the tunnel and ending in the shaft (see Figure 30)
- Air pocket with both head and tail in the tunnel. (see Figure 29)

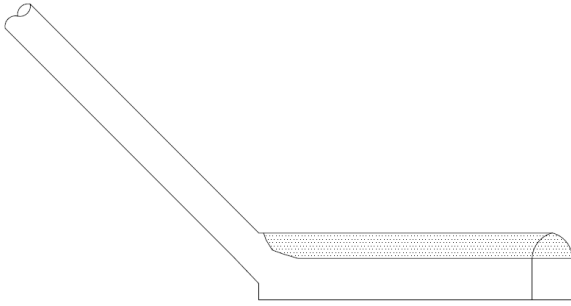


Figure 29-Standing pocket in the tunnel

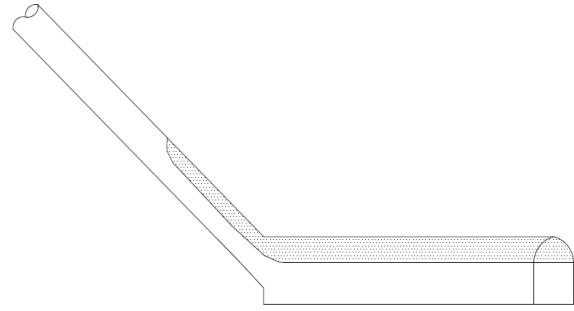


Figure 30-Standing pocket expanding to the shaft

Measurements showed that the pocket thickness in the tunnel was increasing with the rising water discharge. In the setups with 45° and 60° inclined shafts the pocket in the tunnel would grow to a thickness determined by the discharge and further addition of air resulted in pocket expanding into the shaft.

In the 60° shaft for discharge above 35 l/s, the water running under the pocket would act as a jet hitting the bottom of the tunnel. This would create a void from the roof to the floor of the tunnel which was filled with air as seen in Figure 31.

In the 90° setup, the running water was filling the entire cross-section of the shaft and it was entering the tunnel as a jet. The pocket thickness would become bigger with rising discharge eventually filling the space around the jet as seen in Figure 32.

In the experimental setup, the length of the air pocket was limited by the tunnel length and inclination in the model. In the real-world situation, most probably, the air pocket would have a much larger length.

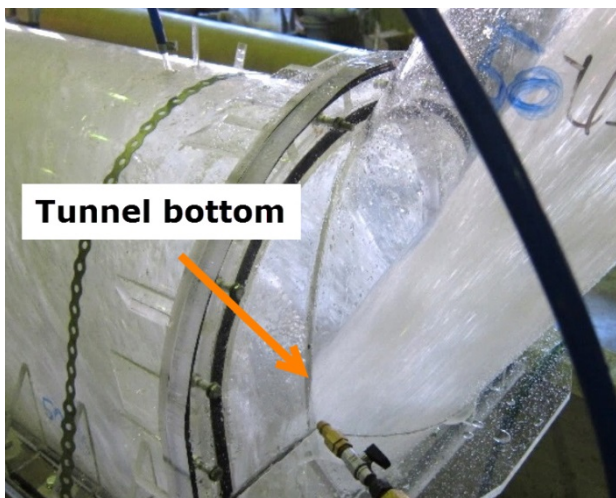


Figure 31- Air accumulation in tunnel with 60° shaft



Figure 32- Air accumulation in tunnel with 90° shaft

4.3.3 Bubble zone

The observations of bubble zone confirmed patterns described by Berg (1986). The air entering the tunnel was dispersed in form of small bubbles. Large turbulences caused by the change in water direction and velocity created a visible whirl and return flow just on the entrance to the tunnel as indicated by Berg. Air travelled further to the tunnel and the bubbles rose to the ceiling. The length of the bubble zone length would rise with the rising discharge.

4.4 Determining dimensionless velocities

During the experiments, it was not observed that standing pocket in the shaft would move downstream. The only possibility for the pocket to be removed from the shaft was by erosion.

For the purpose of the experiment dimensionless velocities were defined as:

- Critical velocity defined here as the velocity at which the pocket would become standing in the shaft (determined from characteristic discharge).
- Threshold flow velocity for continuous air return determined from the measurement of discharge magnitude for which the pocket extending from the tunnel to the shaft would become stationary but never grow to the top of the shaft.
- Clearing velocity was defined as a velocity for which pocket would shrink and move back to the tunnel when air provision was stopped.

4.4.1 Critical velocity

For any given shaft dimension a critical velocity was determined from the flow discharge at which the pocket would become standing in the shaft. The flow conditions in the tunnel had no influence on the standing pocket. Based on the observations the following critical velocities were determined:

Table 8-Determined values for critical velocity

	Critical velocities		
degree	45 ⁰	60 ⁰	90 ⁰
$\frac{v}{\sqrt{gD}}$	0.9	1	0.85

In the setup with the 45⁰ shaft the pocket became standing in the shaft either when the returning smaller air bubbles merged into a larger pocket or if a bigger pocket would start traveling from the tunnel. If air was continuously provided, the pocket would not disappear

for a longer time. When more air was provided, the pocket would first connect to the pocket expanding from the tunnel then it would eventually expand further into the shaft.

In the setup with the 60° shaft the pocket would become standing in the shaft only when air traveled as a pocket from the tunnel. The pocket would not be eroded entirely for a long time if fed by smaller bubbles from upstream or returning from the tunnel. When more air was provided, the pocket would connect to the pocket expanding from the tunnel and finally could expand to the top of the shaft.

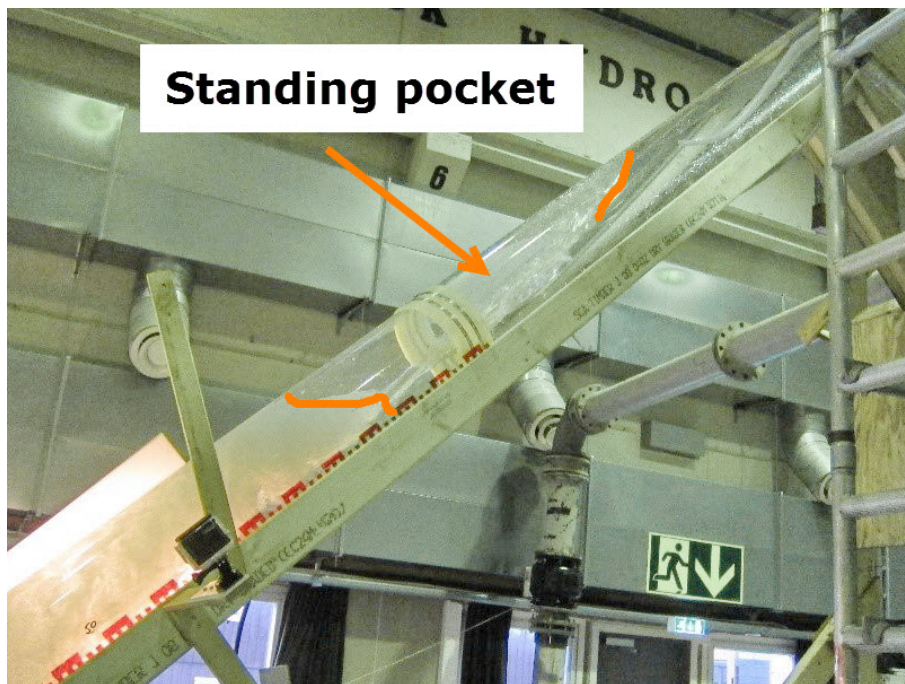


Figure 33- Standing pocket in 45° shaft

Finding a moment for which the pocket would become standing in the vertical shaft was difficult. Since the pocket had no possibility to resist on the ceiling the pocket would never become completely standing but rather moving up and down. It was decided to determine the critical velocity for a situation when the pocket would travel upstream but never reach the top. The pocket would erode fast and the air would disappear to the tunnel. When more air was provided nothing happened to the pocket in the shaft, but the next one traveling upstream would have a larger volume.

The determined values of critical velocity correspond relatively well to the theoretical results yielded by the Kent's equation. The comparison of the determined experimental critical velocities with theoretical velocities yielded by the improved by Wisner version of Kent's equation (equation 9) are presented in Figure 34. Kent experiment was the only one found in

literature which included measurements for 60° slopes. For shaft inclinations 45° and 60°, data determined from the model-observation are consistent with the plot of Kent's equation. The equation predicts a slightly higher critical velocity for angle 60° than for 45° which was confirmed in the model. Plot of Kent's equation indicates further rise of the critical velocity for the 90° shaft. The value determined in the experiment is however much lower. Kent's experiments did not include a measurement for a vertical shaft and the obtained plot shows extrapolated values for this shaft inclination.

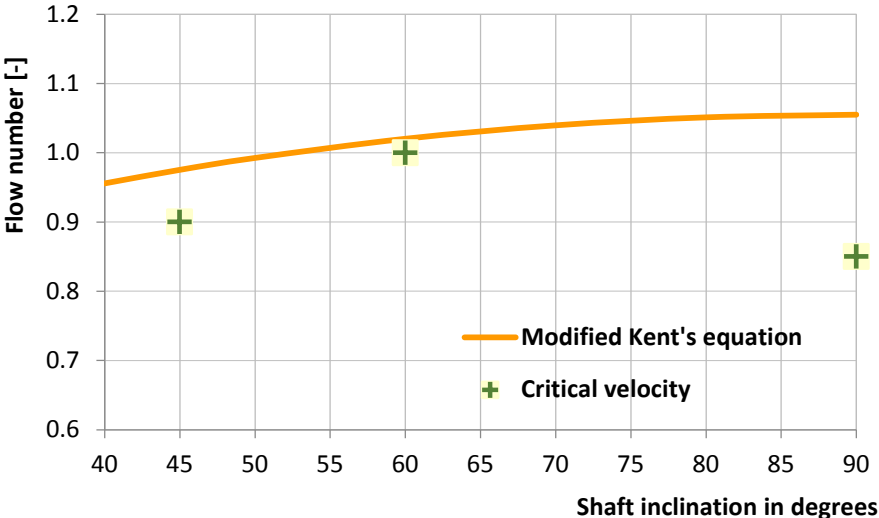


Figure 34-Comparisson of critical velocities determined in the experiment with Kent's equation

4.4.2 Threshold flow velocities for continuous air return

The threshold flow for continuous air return was determined by observation of flow conditions for which the pocket extending from the tunnel to the shaft would become stationary but never grow to the top of the shaft. Experimental results yielded the following dimensionless threshold flow velocities:

Table 9-determined values for threshold flow velocities for continuous return

degree	Threshold flow for continuous air return		
	45°	60°	90°
$\frac{v}{\sqrt{dD}}$	1	1.05	0.9

In shaft with inclination of 45° , the pocket would build up and expand to the tunnel when air was introduced into the tunnel at the flow of 50 l/s that corresponds to Flow Number equal to 1. Sometimes the pocket would detach and travel upstream and become standing in the shaft. When air was introduced upstream at first, several smaller pockets moved upstream and accumulated into a larger standing one in the shaft. For both situations further adding of air resulted in the merge of the pocket in the shaft with the one extending from the tunnel. When more air was provided, the pocket expansion would stop at a certain height in the shaft, and the pocket would never reach the tank.



Figure 35-Pocket reaching the tank, 60° , 50l/s

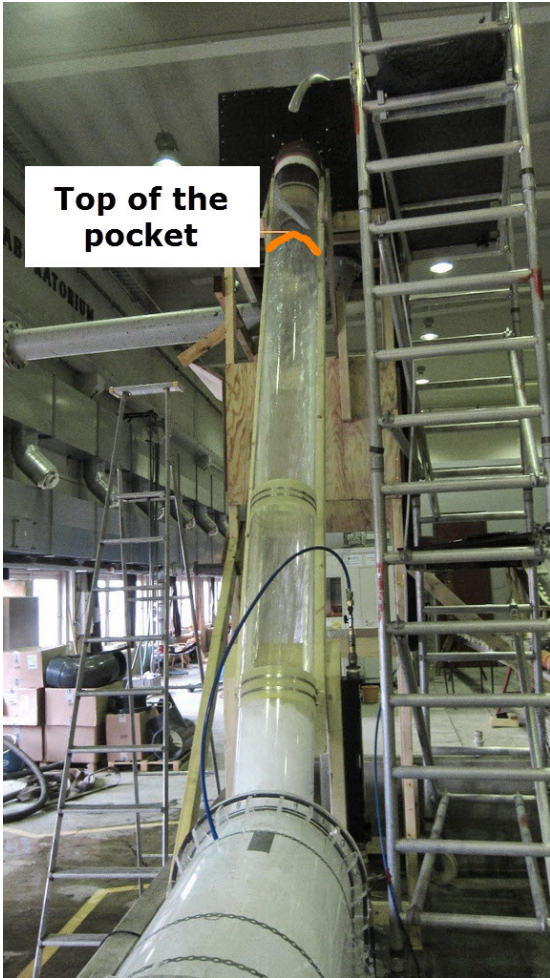


Figure 36-Pocket standing in the shaft, 60° , 55l/s

In the 60° inclined shaft for a discharge of 50 l/s formation of first air pockets was noted in the upper part of the shaft. Addition of more air resulted in merger of the air pocket from the shaft with the pocket expanding from the tunnel. Provision of additional air led to pocket expansion further upstream, and finally, the pocket head would reach the tank as seen in Figure 35. For discharge of 55 l/s ($F=1.1$) the standing pocket head never reached the top of the shaft, this situation is presented in Figure 36.

The determined threshold flow velocities for the model with a 45° inclined shaft confirm the results reported by Berg (1986) and Guttormsen (1986) summarized in Figure 11 and Figure 12 respectively. Results obtained for 90° were also close, while the slight difference can be caused by the much smaller diameter (59 mm) of the shaft pipe used by Guttormsen.

The main conclusion of Gjerde (2009) was that for a conduit inclination of 45° air pockets could still expand to the shaft for $F > 1.35$ which is much higher Flow number value than the value determined in this experiment ($F = 1$). This difference comes from the fact that Gjerde determined the threshold flow for continuous air return for the condition when the air pocket would not expand to the shaft. This assumption is closer to the definition of the clearing velocity used in this work.

4.4.3 Clearing velocity

Clearing velocity is a velocity of the flow needed to transport air pocket to the bottom of the shaft. Clearing velocity was defined in the present experiment as a velocity for which pocket would shrink and move back to the tunnel when air provision was stopped. For the shaft inclination of 90° the clearing velocity was determined in relation to the flow discharge for which a pocket would not appear in the shaft.

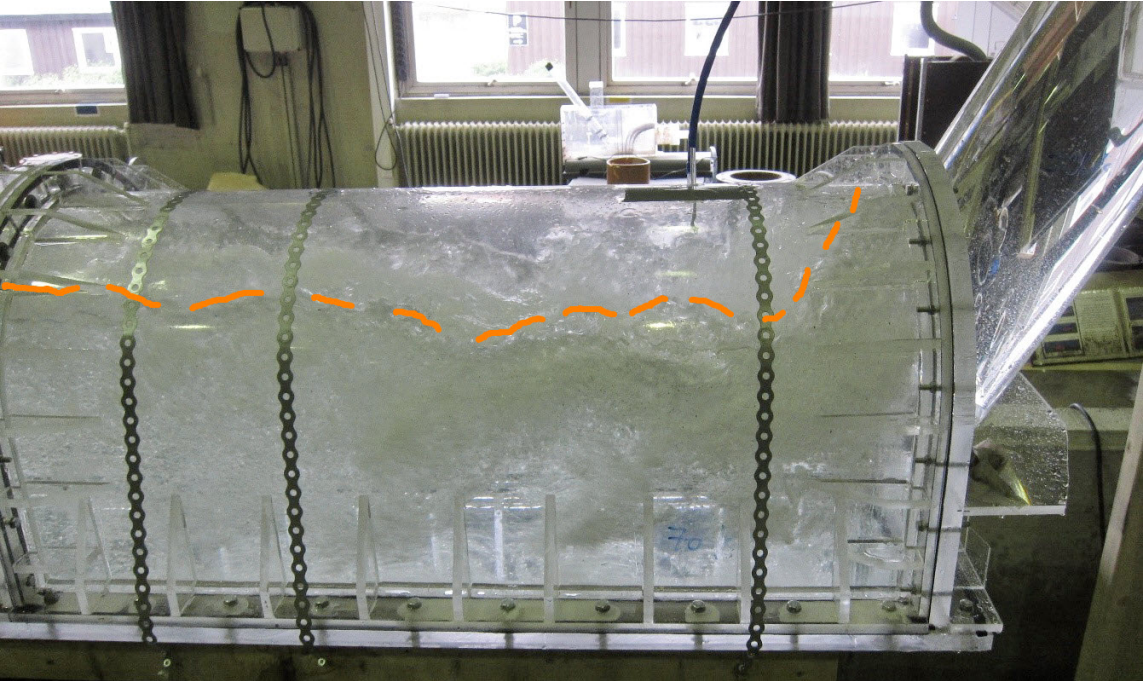


Figure 37-Pocket standing in the tunnel in 60° shaft, $F=1.4$

Based on the observation the following clearing velocities were determined,

Table 10-determined values for clearing velocity

degree	Clearing velocities		
	45 ⁰	60 ⁰	90 ⁰
$\frac{v}{\sqrt{dD}}$	1.3	1.4	1

The clearing velocities determined in the model have relatively large values. This is due to the fact that the earlier experiments carried out to determine this parameter were performed in a conduit with a constant cross-section area (Lubbers, 2007), (Pozos, et al., 2010). The change of the conduit cross-section in the model results in much smaller velocity in the tunnel which creates favorable conditions for the pocket to accumulate in the transition section between the shaft and tunnel. A direct comparison of the obtained results with the results reported in the literature is difficult because of the influence the flow conditions in the tunnel have on the pocket expanding to the shaft.

4.5 Comparison of Flow numbers for different model setup

The comparison of dimensionless velocities determined for the flow in the shaft is presented in Table 11.

Table 11-Summary of determined dimensionless velocities

Inclination	Critical velocity		Threshold flow for continuous air return		Clearing velocity	
	Q [l/s]	F [-]	Q [l/s]	F [-]	Q [l/s]	F [-]
45 ⁰	45	0.9	50	1	65	1.3
60 ⁰	50	1	55	1.1	70	1.4
90 ⁰	42.5	0.85	45	0.9	50	1

The main difference between the various model setups was the change of the shaft inclination. The shaft length also changed for higher inclinations and became shorter. For all three shaft inclinations the determined values of critical, clearing and threshold flow velocity for continuous air return follow the relationship:

$$F_{\text{clearing}} > F_{\text{continuous return}} > F_{\text{critical}}$$

The results also show that each of the determined Flow numbers increase between 45° and 60° shaft inclinations and thereafter start to decrease to a minimum for 90° shaft inclination.

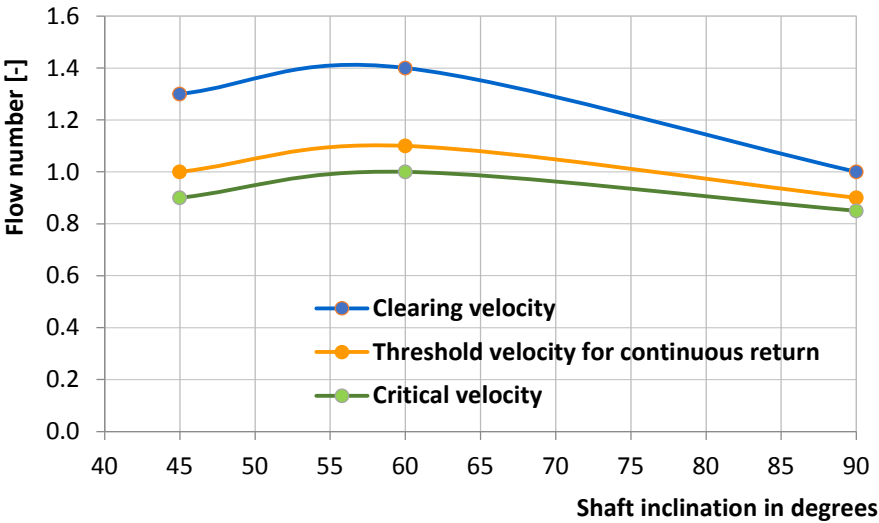


Figure 38-Dimensionless velocities depending on slope of the shaft

Flow numbers are influenced by the pocket head area (Ap), on which the flow acts and their magnitudes. Depending on the shaft inclination they exhibit the following relation:

$$F^{90} > F^{45} > F^{60}$$

Change of the conduit inclination will result in different pocket shapes. In the vertical shaft the pocket will tend to be short and thick while in the 60° shaft the pocket will be long and thin (see Figure 39). The area on which the flow acts is largest for the pocket in a vertical shaft and smallest for the 60° shaft.

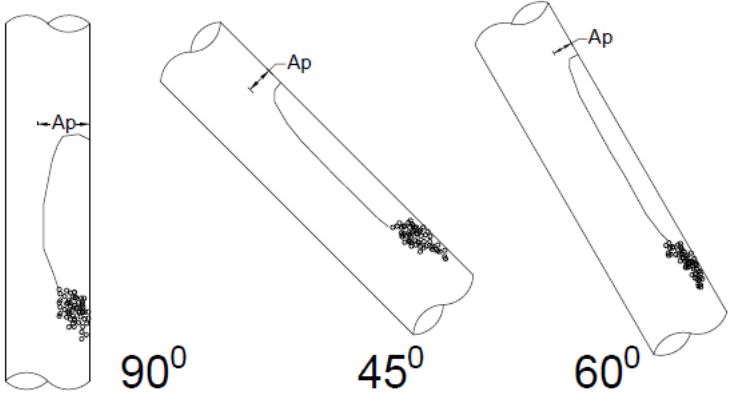


Figure 39-Shape of air pocket depending on the shaft inclination

4.6 Scaling of results

The threshold velocities determined in the experiment were scaled to other shaft dimensions with respect to Froude scaling law, using the formula 15.

$$v_p = v_m \left(\frac{D_p}{D_m} \right)^{1/2} \tag{15}$$

The results of scaling are three curves for different shaft inclinations, determining the maximal flow velocity occurring in the shaft for which the air can return continuously. These curves are presented as solid red lines in Figure 40, but the velocity in the conduit is expressed in relation to discharge.

In addition, the dimensionless velocities for which the air starts to accumulate in the tunnel have been scaled with use of the same method. Resulting curves for different shaft inclinations are presented with dashed blue lines.

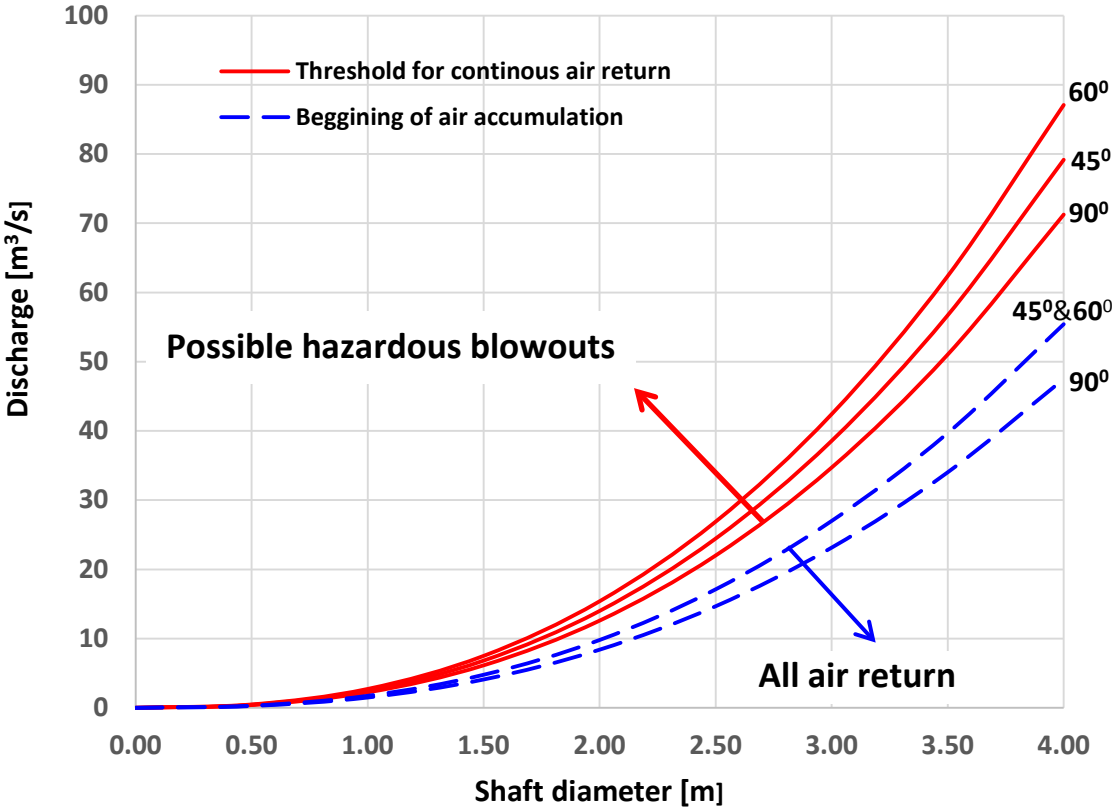


Figure 40 Threshold for continuous air return in the inclined shaft and beginning of air accumulation in the tunnel

For a given shaft diameter and inclination, if the discharge is higher than the one indicated by the corresponding blue dashed curve, there is a possibility for air accumulation in the tunnel

and occurrence of pockets in the shaft. If the discharge is higher than the one indicated by the corresponding red solid line, the air has no possibility to return. This situation can result in a violent blowout.

The outcomes of the laboratory tests are corresponding with the results of previous experiments performed by Berg (1986) and Guttormsen (1986). The present experimental setup has been extended and covers shafts with inclinations 45° , 60° and 90° . It is believed that the results are correct and therefore the graph presented in Figure 40 can be used for estimation of the behavior of the air in the sloped conduits.

4.7 Comparison with prototypes

One of the brook intakes having severe problems with blowouts is the Holmaliåna intake pictured in Figure 1. The shaft at Holmaliåna intake is 48° steep. A long-time monitoring of precipitation, pressure and water stage measurements has been performed by the owner in response to the blowout problems. A sample of these data is presented in Figure 41. The graph illustrates measurements of water elevation with blowouts visible as rapid changes.

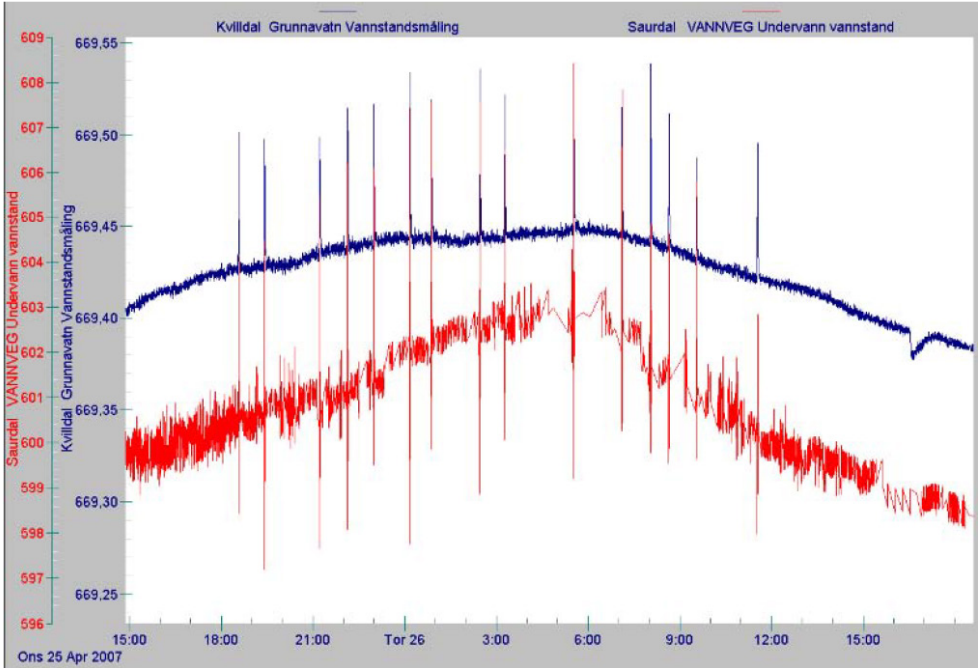


Figure 41- Blowout monitoring at Holmaliåna (Utvik Gjerde, 2009)

Gjerde (2009) analyzed stream flows at Holmaliåna covering the Flow numbers within the range from $F=0.55$ to $F=0.8$. The main conclusion of Gjerde was that the blowouts at Holmaliåna could occur for flow condition when $F>0.6$.

The present experiment for the 45° inclined shaft showed that the air accumulation and occurrence of air pockets in the tunnel starts at Flow number $F=0.7$. This value is close to the results of Gjerde's analysis.

Based on the experiment observations, for a 45° shaft, the threshold velocity for continuous air return was determined to have $F=1$. Frequent occurrence of blowouts at Holmaliåna for $F<1$ indicates that blowouts can occur already at the beginning of air accumulation in the tunnel. Blowouts occurring at Holmaliåna for Flow number $F=0.6$ according to the currently used guidelines are classified as small and not harmful. Whether blowouts of this size are actually dangerous would need to be confirmed with observations on site.

4.8 Test method review

Observation was the primary data collection method in the experiment. The uncertainty of the results is believed to be within acceptable range. Largest inaccuracies may be connected to the volume of air provided to the model due shifting volume of air pumped by the compressor. Water discharge could vary slightly over the time because of the instabilities in the system. Use of a simple video capture method and measurements of air pockets dimensions with a measuring tape are believed to be sufficiently accurate. Air pockets in the model were clearly visible through the pipe therefore, observing the air behavior was possible. The pockets in the shaft moved in a chaotic way simultaneously being eroded. Hence, determining an exact value for return frequency was rather difficult. For larger discharges the thickness of the pocket in the tunnel would allow the air to escape through the outflow.

Rising air that reached the top of the shaft could not leave the model through the intake. For lower discharges below critical velocity, air would rise to the top of the shaft and accumulate in the bend. In this situation, it was necessary to remove this air from the shaft or stop the measurement.

The maximum water head possible to obtain in the model was 280 cm. The model was not able to deliver a compression factor and simulate the expansion of the travelling pocket occurring in the prototype. This model deficiency is likely to have a major impact on the pockets already traveling upstream but it is believed to have much less significance for investigations of standing pockets in the bottom of the shaft.

Berg assumed that providing air in volume equal to 1.3% of the water discharge generates flow conditions occurring in the bottom of the shaft. This assumption was accepted for the

purpose of the experiment. Using a constant air to water discharge ratio gave a possibility to observe the air behaviour in the shaft and tunnel for different water discharges. The actual air amount entrained in the prototype is however unknown.

5 Conclusions

5.1 Final conclusions

It is believed that despite its shortcomings, the experimental model provided interesting results and allowed for verification and better understanding of complex processes related to air-water flow in inclined shafts.

A prerequisite for a blowout to occur is a change of flow regime and formation of air pockets in the intake shaft. This happens for conditions at which air can accumulate in the tunnel.

For all shaft inclinations, from 45° to 90° , the experiment showed that blowouts could occur for discharges much smaller than those indicated by the threshold flow velocity. The intensity of these blowouts (small/large) could not be assessed by the experiment and must be verified in full scale prototype measurements.

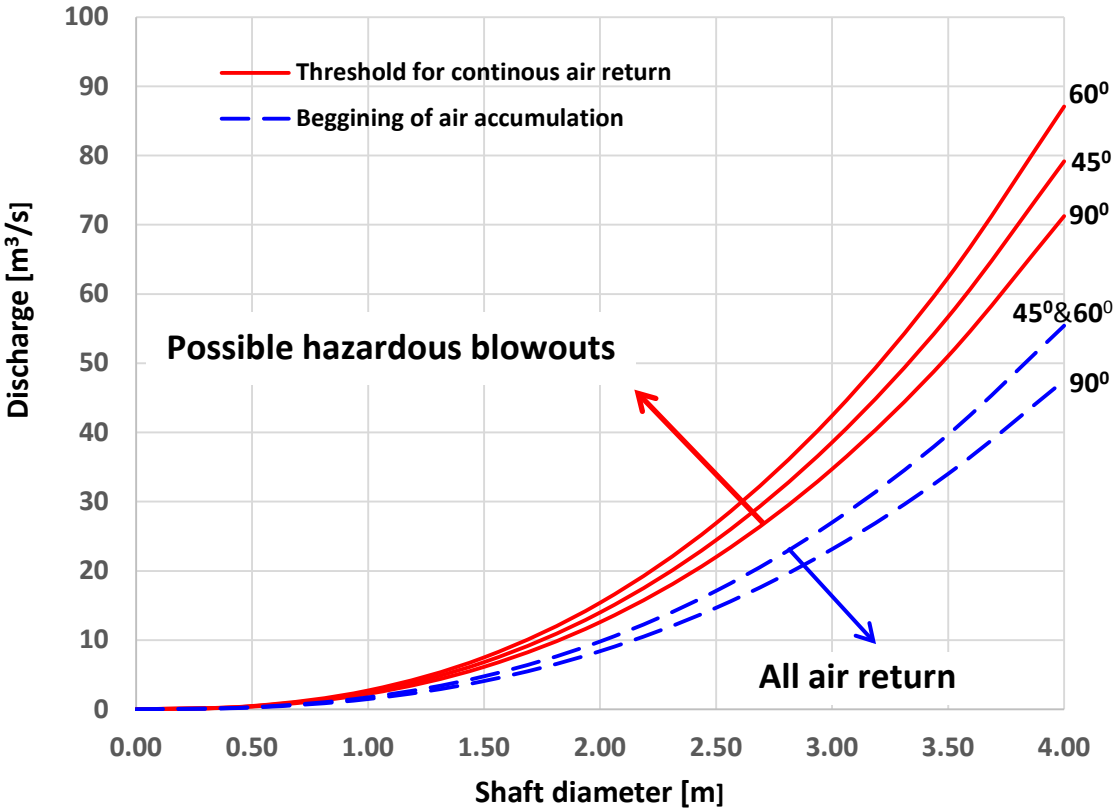
Investigations of standing pockets for the shafts with inclinations of 45° and 60° showed that the pocket in the tunnel will have a limited thickness depending on the discharge while the pocket in the shaft can extend further into the shaft. This observation can lead to a conclusion that larger blowouts are associated with the air accumulation in the shaft.

From the observations it can be concluded that the source of larger air volumes is more likely to be from entrainment in another brook intake in the system than from the considered intake itself. Potential for accumulation of larger air volumes ergo larger blowouts is higher when the air comes from the tunnel side.

For inclination setup of 45° the waves occurring in the tunnel would often push the standing pocket into the shaft. This traveling wave is believed to have a potential to trigger a blowout and to create oscillations in the system. This situation was neither observed in the setup with a 60° or in the setup with 90° shaft.

In vertical shaft the air accumulation in the tunnel and formation of air pockets in the shaft would start at much lower discharges compared to the 45° and 60° shafts. Entrainment of air from upstream prevented pockets return up the shaft and resulted in air accumulation in the tunnel. When the air provision was reduced, larger pockets would start traveling upstream. It is believed that in a full scale design this mechanism could lead to a violent blowout.

The outcomes of the laboratory tests are corresponding with the results of previous experiments performed by Berg (1986) and Guttormsen (1986). The present experimental setup has been extended and covers shafts with inclinations 45° , 60° and 90° . It is believed that the results are correct and therefore the threshold curves presented in the figure below can be used to predict air behavior in inclined shafts and help in design of brook intakes.



5.2 Recommendation for further research

Vertical shaft

Experiment performed in this project showed a substantial difference in the behavior of air in the 90° inclined shaft as compared to the 45° and 60° inclined shafts. It was observed that for the vertical model setup the air entrained into the shaft prevents air pockets from returning up the shaft. This situation is considered to be hazardous. Further research of this phenomena and more detailed studies of the flow in the vertical shaft should be carried out.

Air entrainment

The experiment showed that the amount of entrained air has a significant influence on the air behavior in the closed water conduits. Berg assumed that a constant air to water ratio of

1.3% represents the air-water flow conditions in a bottom of the shaft. Berg assumption should be confirmed since the actual/exact air-water ratio is unknown. To allow for further research, more data on air entrainment need to be collected from prototypes.

Blowout mechanism

Experimental method was used several times in Norway to study blowout mechanism in brook intakes. However, results obtained in the laboratory do not match the prototype behaviour and the mechanism of the blowouts in the real world is still little known. The outcomes of laboratory studies are affected by the limited water head which can be obtained in the model. High pressure occurring in the prototype leading to compression of the air is believed to be the most influential factor that intensifies blowouts. In order to enhance knowledge on blowouts mechanism it is crucial to investigate this phenomenon with full scale prototype measurements.

Model improvement

During experiments, no blowout occurred in the model. The reason for this could be an incorrect location of the intake on the side of water tank. It is believed that placing the intake in the bottom of the tank would be a better solution preventing the air from accumulating in the connecting elbow pipe and allowing air to leave through the intake.

6 Bibliography

- Awad, M. M., 2012. Two-Phase Flow. In: *An Overview of Heat Transfer Phenomena*. s.l.:InTech.
- Bekkeinntakskommiteen, 1986. *Bekkeinntak på Kraftverkstunneler, Sluttrapport fra Bekkeinntakskommiteen*, s.l.: Vassdragsregulantenenes Forening.
- Berg, A., 1986. *Modellforsøk av tofase luft-vann-strømning i bekkeinntakssjakter*, s.l.: Norsk hydroteknisk laboratorium.
- Dahl , R. & Guttormsen, O., 1986. *Direkte innføring av bekkeinntakssjakt på driftstunnel - modellforsøk*, s.l.: Norges Hydrotekniske Laboratorium.
- Ervine, D. A., 1998. *Air entrainment in hydraulic structures:a review.*, s.l.: Proceedings of.
- Escarameia, M., 2006. Investigating hydraulic removal of air from water pipelines. *Water Management 160(WMI): 10*.
- Falvey, H. T., 1980. *Air water flow in hydraulic structures*, s.l.: Water and power Resources Services, Engineering and Research Center.
- Gandenberger, W., 1957. *Über die Wirtschaftliche und betriebssichere Gestaltung von Fernwasserleitungen*, Munchen: R. Oldenbourg Verlag.
- I. Pothof, F. Clemens, 2008. On gas transport in downward slopes of sewerage mains. *11th International Conference on Urban Drainage, Edinburgh, Scotland, UK, 2008*.
- Kalinske, A. A. & Bliss, P. H., 1943. Removal of air from pipe lines by flowing water. *Proceedings of the American Society of Civil Engineers (ASCE)*, 13(10).
- Kent, 1952. *The entrainment of air by water flowing in circular conduits with downgrade slope*, Berkeley, California: s.n.
- Lubbers, C. L., 2007. *On gas pockets in wastewater pressure mains and their effect on hydraulic performance*, Delft: Delft University of Technology.
- Palsson, H., n.d. *Two phase flow – flow regimes*, s.l.: University of Iceland.
- Pothof, I. W. M., 2011. *Co-current air-water flow in downward sloping pipes*, Delft: Technical University Delft.

Pozos, O. et al., 2010. Air entrapped in gravity pipeline systems. *Journal of Hydraulic Research Vol. 48, No. 3*, pp. 338-347.

Utvik Gjerde, R., 2009. *Luftproblem i bekkeinntak*, s.l.: Masteroppgave ved NTNU.

Weisman, J., 1983. Two-phase flow patterns. Chapter 15. In: *Handbook of Fluids in Motion*. s.l.:Ann Arbor Science Publishers.

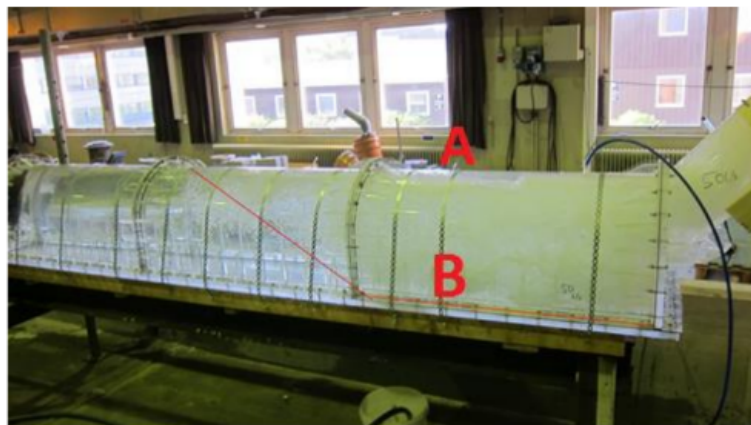
Yang, J. & Liu, T., 2013. Experimental studies of air pocket movement in a pressurized spillway conduit. *Journal of Hydraulic Research*, 51(3), pp. 265-272.

Zukoski, E., 1966. Influence of viscosity, surface tension and inclination on motion of long bubbles in closed tubes. *Fluid Mech.*, Volume 25(4), pp. 821-837.

Appendix A- Example of observations for 45⁰ shaft

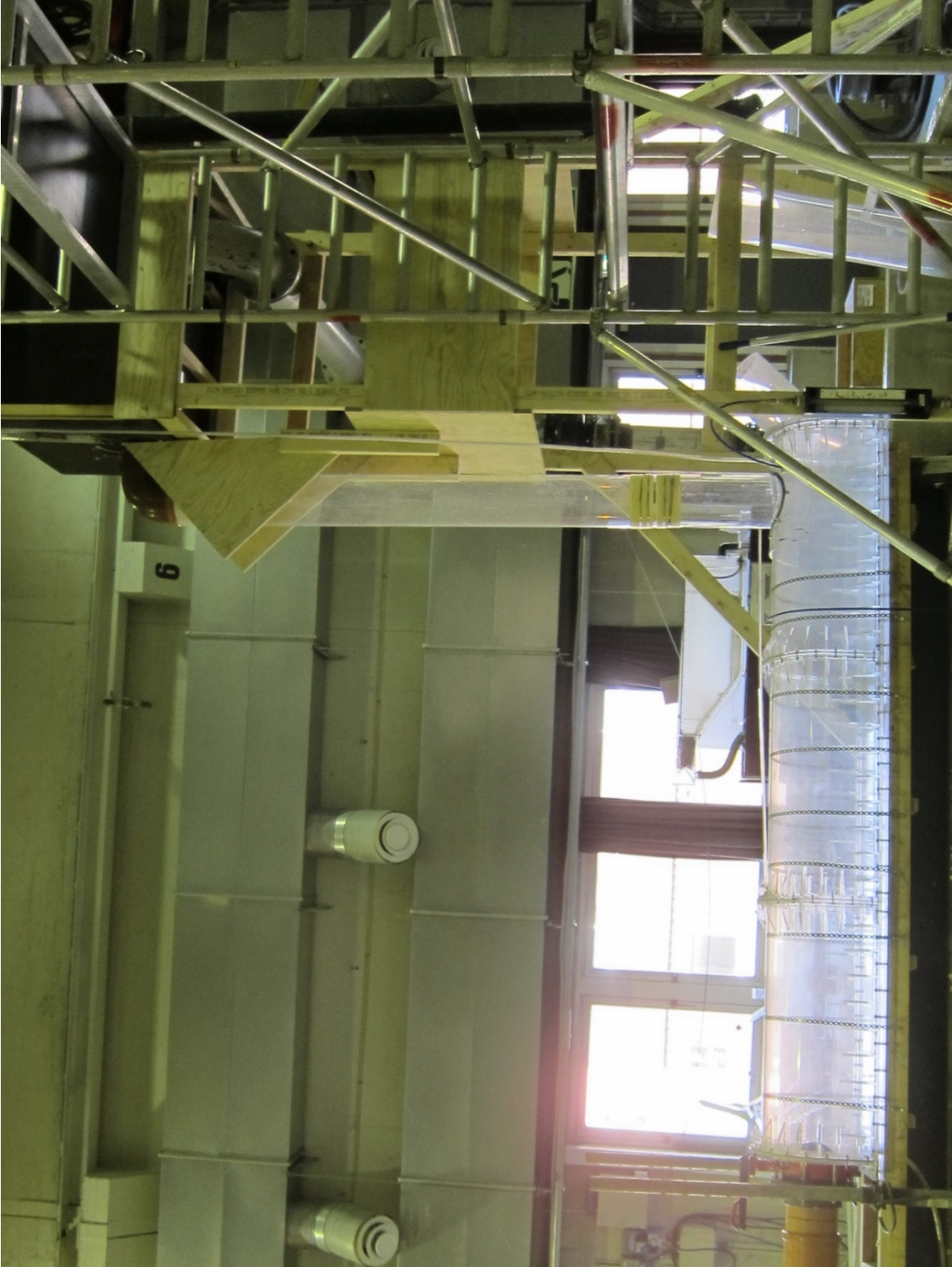
Discharge	v/gD	Frequency of return for air introduced in:		Bubble zone length		Pocket height
		Tunnel	Shaft	a	b	
l/s	[-]	ret/min	ret/min	cm	cm	cm
20	0.4	50	x	x	x	x
Observations: <ul style="list-style-type: none"> No pocket formation All air returned upstream. Air introduced in the shaft didn't reach the tunnel. 						
25	0.4	40	70	x	x	x
Observations: No pocket formation All air returned upstream Air introduced in the shaft didn't reach the tunnel						
30	0.6	25	50	80	50	x
Observations: <ul style="list-style-type: none"> No pocket formation All air returned upstream. Only part of the air introduced in the shaft reached the tunnel 						
35	0.7	18	43	90	55	1
Observations: <ul style="list-style-type: none"> All air returned upstream. For air introduced to the tunnel: <ul style="list-style-type: none"> Air accumulation in the tunnel Air returns as large bubbles For air introduced to the shaft: <ul style="list-style-type: none"> No air accumulation in the tunnel Returning bubbles are small 						
40	0.8	15	40	100	60	3
Observations: <ul style="list-style-type: none"> All air returned upstream. For air introduced to the tunnel: <ul style="list-style-type: none"> Air accumulation in the tunnel Air returns as large bubbles For air introduced to the shaft: <ul style="list-style-type: none"> No air accumulation in the tunnel Returning bubbles are small 						

45	0.9	12	12	130	90	4
<p>Observations:</p> <ul style="list-style-type: none"> All air returned upstream. <p>For air introduced in the tunnel:</p> <ul style="list-style-type: none"> Large bubbles traveling upstream but never became standing in the shaft <p>For air introduced in the shaft:</p> <ul style="list-style-type: none"> Air accumulation in the tunnel Medium size bubbles return 						
50	1	1	1	170	100	6
<ul style="list-style-type: none"> The pocket in the tunnel would always be established. When air was introduced into the tunnel a large pocket would start moving upstream and then become standing When air came from upstream first the pocket was build. Then few smaller bubbles raised and build up a pocket upstream standing. After that for both cases it looks similar. When air was added eventually the pocket in the shaft and in the tunnel, would become one long 						
55	1.1	0	1	105	200	8
<ul style="list-style-type: none"> The pocket would expand in to the shaft and become standing. Additional air provided didn't change the pocket state When air was provided from upstream large pocket would start traveling upstream but eventually become stationary in the shaft. After more air was provided the pocket would merge with the pocket expanding from tunnel 						
60	0	0	0	110	220	11
<ul style="list-style-type: none"> Both for air provided to the tunnel and to the shaft the pocket would only grow and expand from tunnel to the shaft to a certain height and then become stationary. 						
65	0	0	0	x	x	x
<ul style="list-style-type: none"> Pocket would still expand to the shaft 						
65	0	0	0	x	x	x
<ul style="list-style-type: none"> Pocket would expand to the shaft only if constant air was provided 						



Appendix B- Additional model pictures

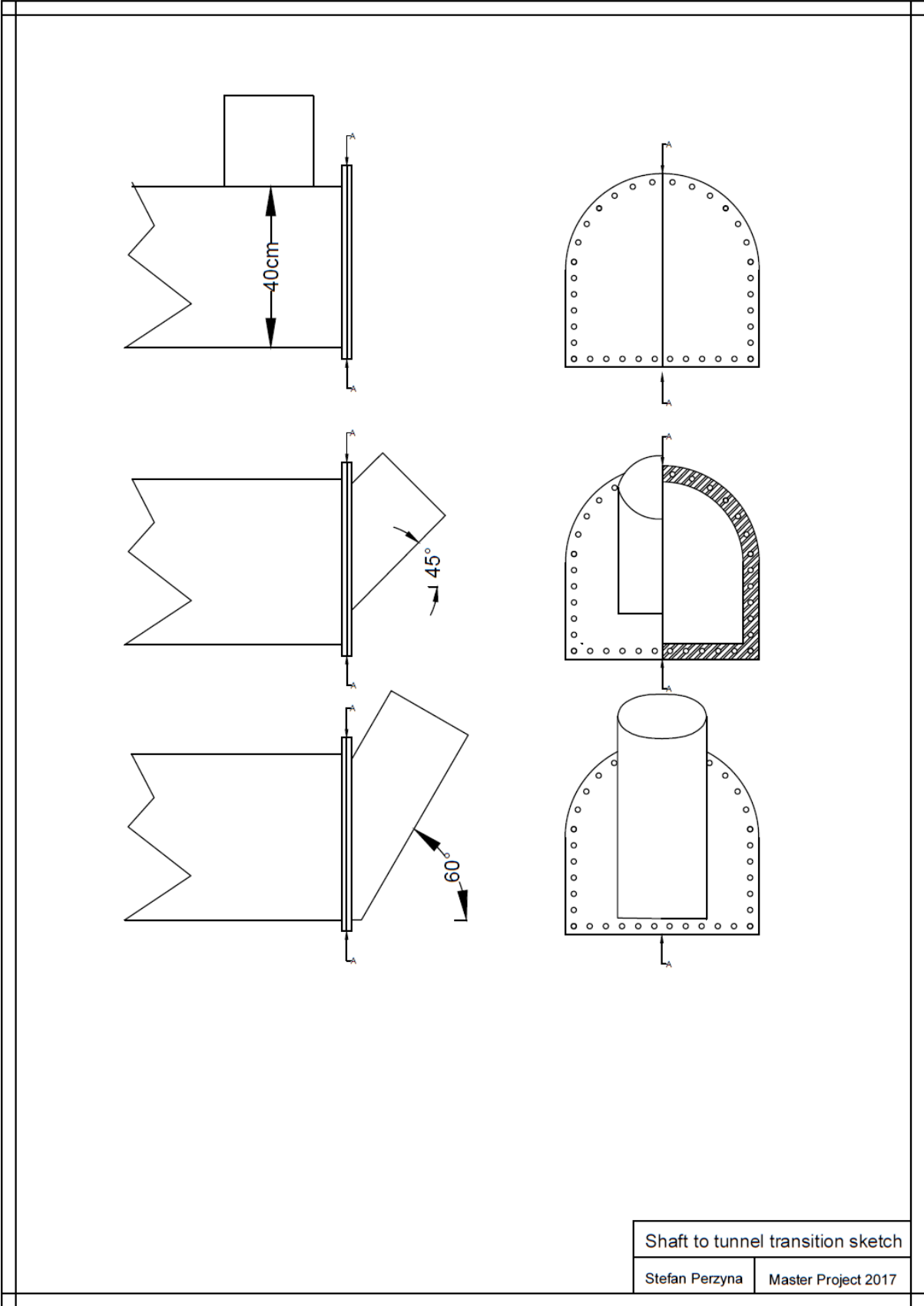
Model with the vertical shaft setup



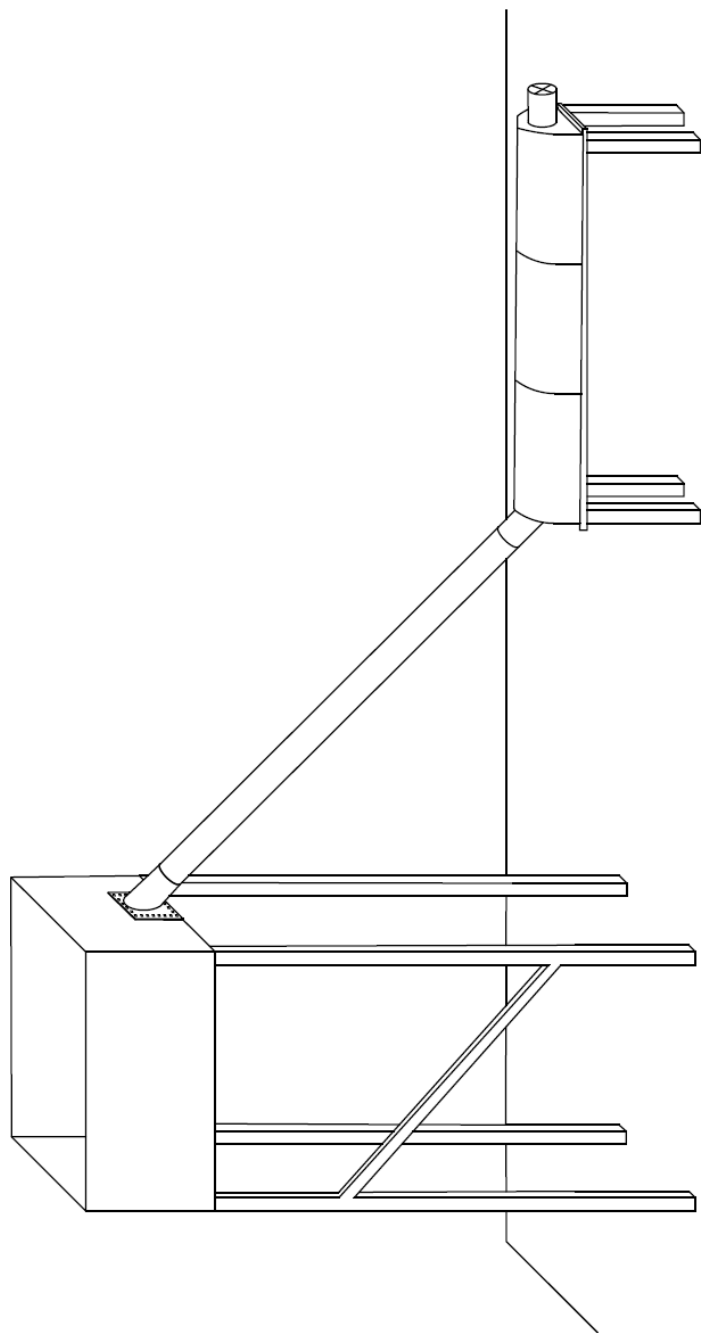
Model with the 60° inclined shaft



Appendix C- Model design sketches



Shaft to tunnel transition sketch	
Stefan Perzyna	Master Project 2017



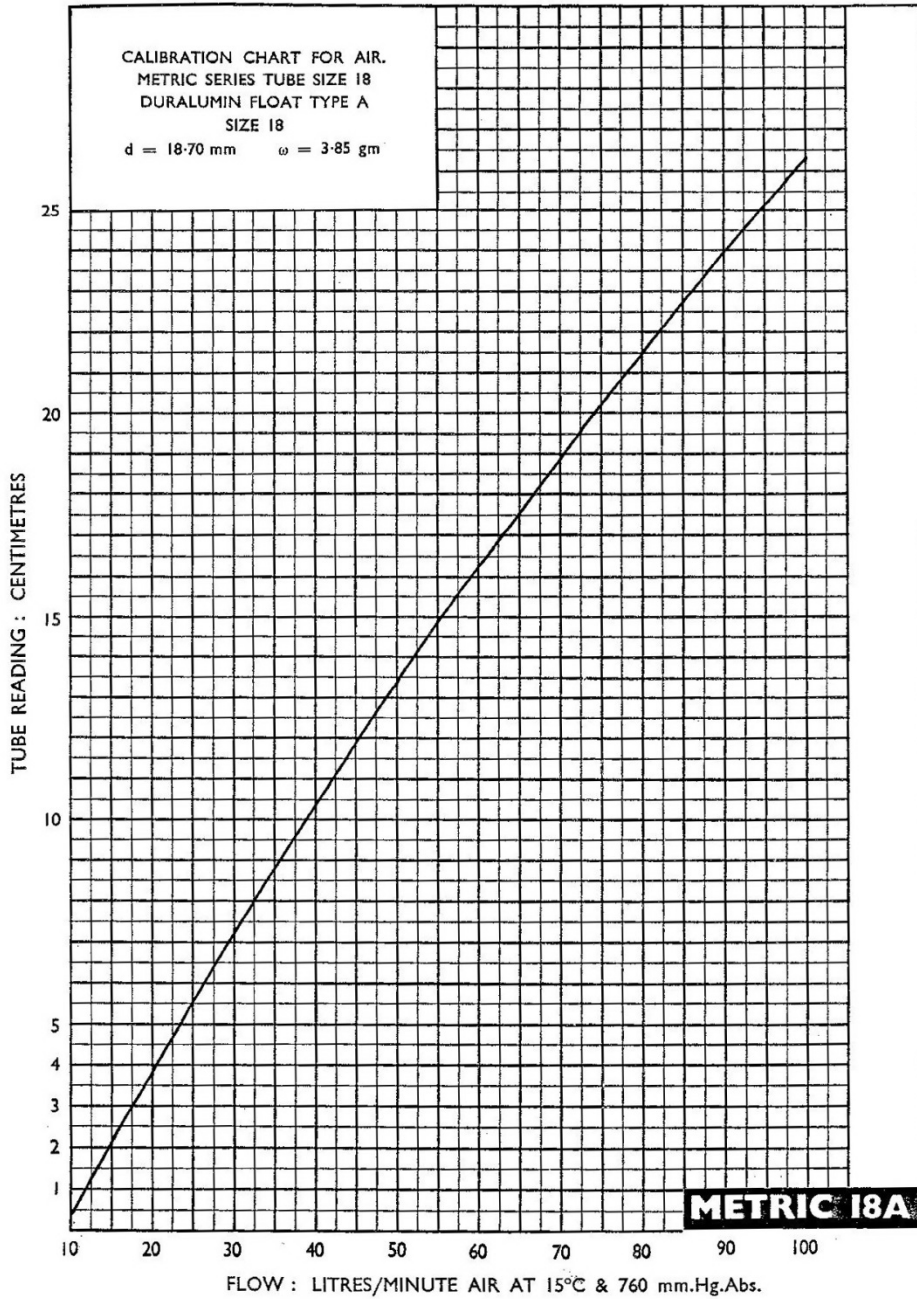
First model sketch

Stefan Perzyna

Master Project 2017

Appendix D- Air discharge curve

ROTAMETER MANUFACTURING CO. LTD., CROYDON, ENGLAND. PUBLICATION No. **RP.2317**



AIR CALIBRATION CHART FOR METRIC SERIES ROTAMETER TUBE SIZE 18 WITH FLOAT TYPE A

Appendix E- Master Thesis contract

NTNU
Norges teknisk-naturvitenskapelige
universitet

Fakultet for ingeniørvitenskap
og teknologi
Institutt for vann- og miljøteknikk



MASTEROPPGÅVE

Student: *STEFAN PERZYNA*

Tittel: **RETUR AV LUFT I BEKKEINNTAKSJAKTER**

1 BAKGRUNN

Når vasskraft skal byggast ut i alpint landskap, vil det ofte bli bygd lange overføringstunnal med mange små inntak, kalla bekkeinntak. Mellom bekkeinntak og tunnel renn vatnet vanlegvis ned ei sjakt eller bratt tunnel, der vatnet vil rive med seg luft. Denne lufta fører til mange ulemper dersom den ikkje handsamast rett. Vanlege ulemper er akkumulering av luft i tunnel med falltap, luftovermetning i nedstraums vassdrag/vatn og til sist skadelege utblåsingar. Det har heilt sidan 80-talet vore kunnskap tilgjengeleg for og i hovudsak unngå problema, men det viser seg enno at mange vannkraftsystem har problem med luft ifrå bekkeinntak. Dei siste åra har det i Noreg vore lite forskning og merksemd rundt luft, sett bort ifrå eit forskingsprosjekt på NTNU i 2009. Det er derfor viktig at denne kunnskapen no trekkast fram i lyset og at gapet mellom teori og observasjonar i felt vert forsøkt lukka.

Hausten 2016 vart det skrive ein prosjektoppgåve om luftmedriving og –utblåsing i bekkeinntak her på NTNU, der det m.a. vart vist samanheng mellom feildimensjonering og utblåsing på heilt nye anlegg. Oppgåva konkluderer også med at det er nødvendig å teste hastighet på bobler i skrå bekkeinntakssjakter, der dette vil ha innverknad på kva slag hydrauliske forhold som må til for at luft skal returnere i sjaktene til kvart inntak.

Det er nødvendig å bygge ein fysisk modell for å kunne studere slik to-fase straum i detalj. Det skal derfor byggast ein modell tilsvarande den som vart nytta under forsøka i Vassdragslaboratoriet i 2009. Oppbygging av modellen er ein del av masteroppgåva.

2 HOVUDPUNKT I OPPGÅVA

Arbeidet vil innehalde følgjande hovudpunkt:

1. Samanstilling av dagens kunnskap om retur av luft i tunnelar og bekkeinntaksjakter.
2. Utarbeiding av modeloppsett
3. Deltaking i bygging av fysisk modell
4. Etablering og gjennomføring av testprogram for retur av luft i sjakter
5. Samanlikning av resultat med tidlegare forsøk og med observasjonar i felt
6. Konklusjon og rapportering

Innhaldet i prosjektet vil bli nærmare avgjort av rettleiar i samråd med samarbeidspartnerar som vil bli knytt til prosjektet.

3 RETTLEIING, DATA OG INFORMASJON

Hovudrettleiar vil vere Professor Leif Lia. Medrettleiarar vert Senioring. Morten Skoglund. Kontaktperson i rådgivarbransjen vert siv.ing. Are Sandø Kiel.

Diskusjon med og bidrag frå kollegaer og medarbeidarar med NTNU, SINTEF, Rådgivande ingeniørfirma og andre firma og organisasjonar vert tilrådd. Bidrag som går inn i oppgåva skal alltid refererast til på rett vis.

4 RAPPORTFORMAT, REFERANSAR OG ERKLÆRING

Oppgåva skal skrivast i eit tekstbehandlingsprogram slik at figurar, tabellar, foto osv. får god rapportkvalitet. Rapporten skal innehalde eit samandrag, ei innhaldsliste, ei litteraturliste og opplysningar om andre relevante referansar og kjelder. Oppgåva skal leverast i B5-format som .pdf i DAIM og trykkast i tre eksemplar som sendast direkte frå trykkeri til faglærer/institutt. Samandraget skal ikkje gå over meir enn 450 ord og skal vere eigna for elektronisk rapportering.

Masteroppgåva skal ikkje leverast seinare enn den leveringsfristen som kjem fram i DAIM (20 veker + offentlege fridagar vårsemesteret).

Trondheim, 16. januar 2017

Leif Lia
Professor